

## 1.1 Straw Tracker

### 1.1.1 Introduction

The purpose of the STRAW Tracker is to measure with good accuracy the direction and the momentum of secondary charged particles originating from the decay region. The spectrometer (see Figure 1) consists of four chambers intercepted in the middle by a high aperture dipole magnet providing a vertical B-field of 0.36T. Each chamber is equipped with 1'792 straw tubes, which are positioned in four "Views" providing measurements of four coordinates (see Figure 2).

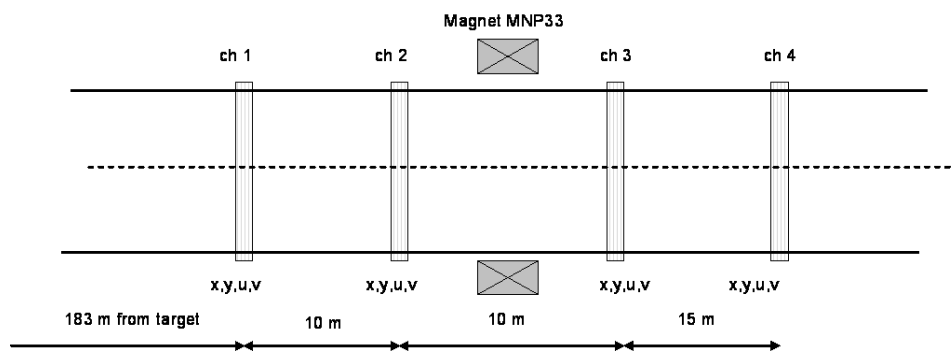


Figure 1. Schematic view of the magnetic spectrometer.

The main building block of the detector is an ultra-light straw tube which is 2.1m long and 9.8 mm in diameter. The tubes are manufactured from 36  $\mu\text{m}$  thin PET<sup>1</sup> foils, coated –on the inside of the tube– with two thin metal layers (0.05  $\mu\text{m}$  of Cu and 0.02  $\mu\text{m}$  of Au) to provide electrical conductance on the cathode. The anode wire ( $\varnothing=30 \mu\text{m}$ ) is gold-plated tungsten.

#### 1.1.1.1 Straw Tracker Detector Requirements

As illustrated in the proposal (1), kinematical constrains in the events allow the rejection of the majority of the background provided the kaon and pion tracks are reconstructed with good accuracy. Two principal performance requirements –for secondary particles– follow from this:

and

<sup>1</sup> PET = polyethylene terephthalate

In addition to the above, it is important to stress that the overall physics performance of NA62 depends on a number of experimental necessities for the Straw Tracker:

- Use of ultra-light material along the particle trajectory in order to minimize multiple Coulomb scattering, in particular, near the first chamber.
- Integration of the tracker inside the vacuum tank.
- An intrinsic spatial resolution that allows a precise reconstruction of the intersection point between the decay and parent particle.
- Average track efficiency near 100%.
- Capability to veto events with multiple charged particles
- Sufficient lever arm between the four chambers allowing to re-use the exiting dipole magnet.

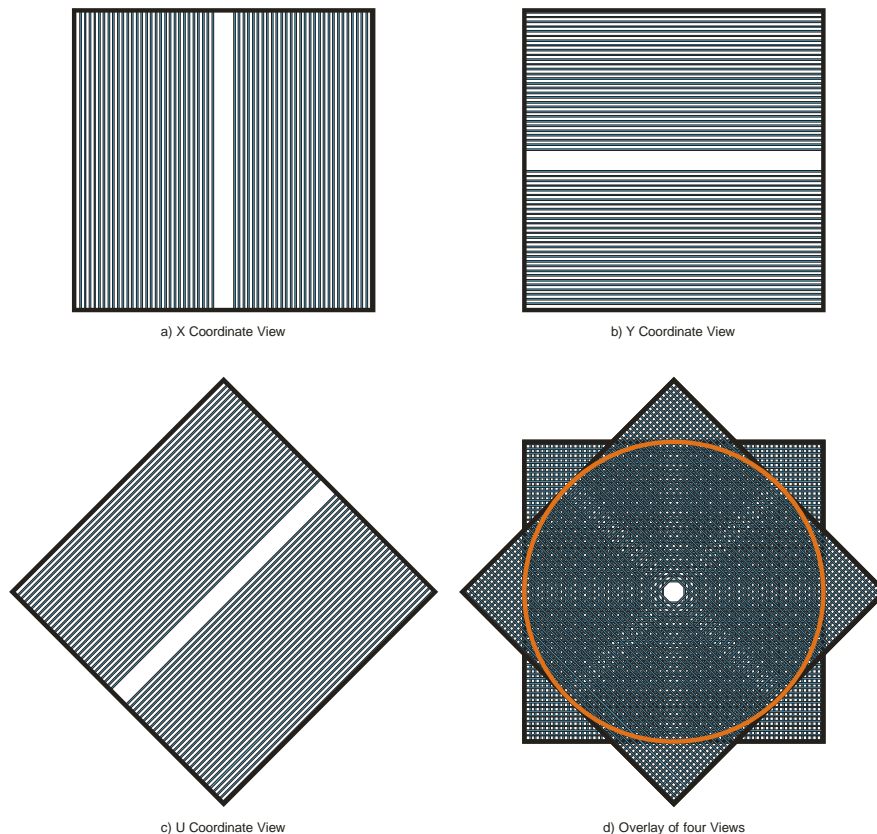


Figure 2. Schematic drawing of the four "Views" that compose each straw chamber. a) the x-coordinate view with vertical straws, b) Y-coordinate View with horizontal straws, c) the U-coordinate view (the V-coordinate view is rotate by 90 degrees compared U-Coordinate), d) A full chambers consisting of the X,Y,U and V Views; the active area of the chamber covers a diameter of 2.1m. The gap near the middle of each layer is kept free for the beam passage.

From these constrains follow the main requirements of the detector:

- Spatial resolution  $\leq 130 \mu\text{m}$  per coordinate and  $\leq 80 \mu\text{m}$  per space point
- $\leq 0.5\%$  of a radiation length ( $X_0$ ) for each chamber
- Installation inside the vacuum tank ( $P = 10^{-5}$  mbar) with minimum gas load for the vacuum system

- For straws near the beam, operation in a high rate environment (up to 40 kHz/cm, and up to 500 kHz/Straw)
- Contribution as multiplicity veto to the trigger

The most important parameters for the straw tracker of NA62 are summarized in Table 1.

Table 1. The main parameters of the straw tracker.

Chamber layout	Value			Comment
Number of chambers	4			Beam shifted towards the Jura side
Number of views/chamber	4			
Number of straw layers/view	4			
Number of straws/view	448			
Central gap	~12 cm			
Central gap off-set vs. beam axis	X	Y	U=V	
Chamber 1	101.2 mm	0	70.4 mm	
Chamber 2	114.4 mm	0	79.2 mm	
Chamber 3	92.4 mm	0	66 mm	
Chamber 4	52.8 mm	0	39.6 mm	
Track angle coverage	$\pm 3^\circ$			Active length
Straw length	210			
Straw position accuracy	$\pm 0.1$ mm			Toshiba
Wire	30 $\mu$ m gold-plated Tungsten			
Straw inner diameter	$9.75 \pm 0.05$ mm			
Straw straightness	$\pm 0.1$ mm			
Maximum wire off-set	0.2 mm			
Gas volume in one straw	160 cm <sup>3</sup>			
<b>Straw material (option 1)</b>				
Mylar film	36 $\mu$ m			
Density	1.39 g/cm <sup>2</sup>			
Copper layer	500 Å			
Gold layer	200 Å			
<b>Material budget ( 1 view)</b>	<b>Radiation length in %</b>			
Gas	0.010			
Straw wall	0.099			
Wires	0.0046			
Total	0.1136			
<b>Straw operating conditions</b>				Inner most straws
Wire tension	(90 $\pm$ 10) g			Option: 90%CO <sub>2</sub> ,5%Isobutan,5%CF <sub>4</sub> Option: 2.5kV
Gas	70% Argon ,30%CO <sub>2</sub>			
High Voltage	1.75 kV			
Gain	$1 \cdot 10^5$			
Cathode resistivity	~70 ohm/			
Max Counting rate/straw	0.5 MHz			
High rate per unit area	40 kHz/cm <sup>2</sup>			Straws close to center gap 50 000 bursts of 3s
Accumulated charge	0.015 C/cm/year			
Maximum current/cm	64 nA/cm			
Gas flow per straw / per view	160 cm <sup>3</sup> /h / 70 l/h			High flow straws
Gas pressure (absolute)	1.02-1.04 bar			
Nominal electron drift time	140 ns			
Nominal ion drift time	100 $\mu$ s			
Effective radius	4.8 mm			>95% efficiency Estimated
Cross-talk	3%			
Nominal threshold	3 fC			5 fC Estimated
Termination resistor (far end)	330 Ohm			

### 1.1.1.2 Simulation of Straw Performance

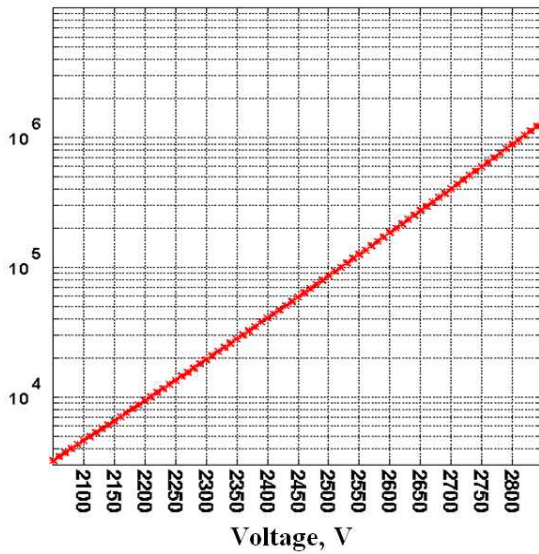
#### 1.1.1.2.1 Track Multiplicity Veto in High Rate Environment

To verify if the straw inefficiency is acceptable for the detector veto function, a fast and simplified Monte Carlo simulation of the possible background decays has been carried out. It was found that an overall inefficiency level of 5% does not lead to a significant change of the three-track veto efficiency with the current detector geometry. Decays like  $K \rightarrow 3\pi^+$  and  $K \rightarrow \pi^+\pi^-\mu^+\nu$  with rather symmetric track distribution (caused by a small amount of kinetic energy), can be easily suppressed by the spectrometer multiplicity veto down to the level of  $10^{-8}$  (limited by the simulated statistics of 100 million decays per mode).

In this respect the decay  $K \rightarrow \pi^+\pi^-\mu^+\nu$  (called Ke4) represents one of the most problematic backgrounds. With a low-energy electron and a negative pion that misses the first three chambers -due to the Straw Tracker beam gap- the veto relies on the measurement in the last Straw Chamber. If the pion is very close to the beam, it can occur that the measurement is done in only one single layer of the last chamber. From fast Monte Carlo simulation one can conclude that if the fourth chamber measures the negative pion from Ke4, with a straw inefficiency of better than 5%, it will suppress this background to an insignificant level.

The biggest track rates are expected on straws located near the beam gaps (Figure 2). Simulations show that the highest peak rates are in chamber 4 on the most inner straws on the Saleve side (positive X). However, more important is the efficiency on the inner straws on the Jura side, where Ke4 negative pions must be detected. Halo simulations, presented in Section **Error! Reference source not found.** on page **Error! Bookmark not defined.**, predict a rate of 0.3 MHz due to kaons and pions inside and outside the fiducial region. Simulations of the other five dominating modes of kaon decays in the beam add another  $\approx 0.08$  MHz. Therefore, one can conservatively estimate the maximum rate for the important straws to be at the level of 0.5 MHz, which gives the final requirement for the straw rate capability. In these conditions the straw efficiency at the straw centre should remain at a level of 95%.

## Amplification



## Amplification

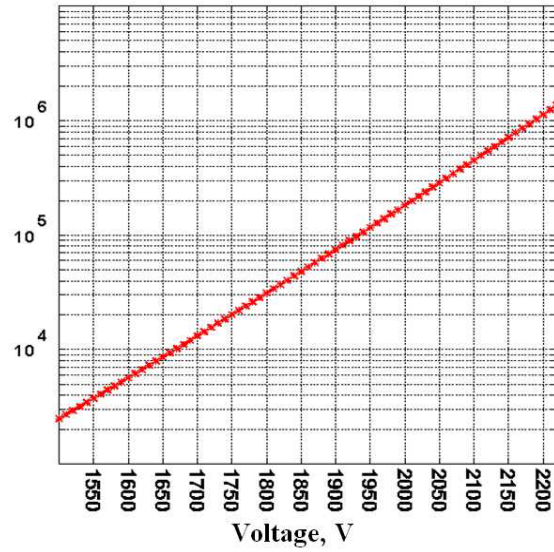


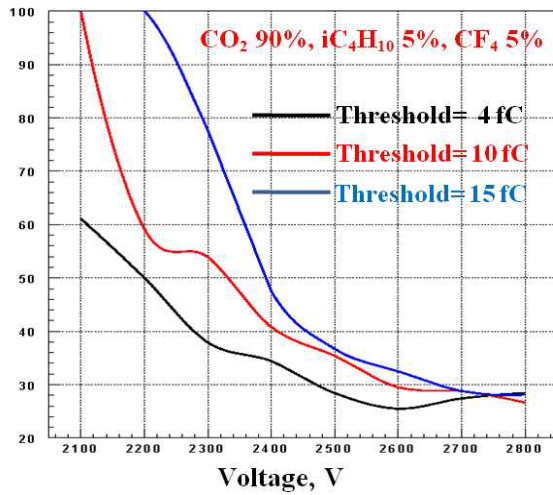
Figure 3. The simulated dependence of the gas gain on the high voltage for gas mixtures CO<sub>2</sub> 90%, iC<sub>4</sub>H<sub>10</sub> 5%, CF<sub>4</sub> 5% (left) and Ar 70%, CO<sub>2</sub> 30% (right).

### 1.1.1.2.2 Spatial Resolution and Efficiency

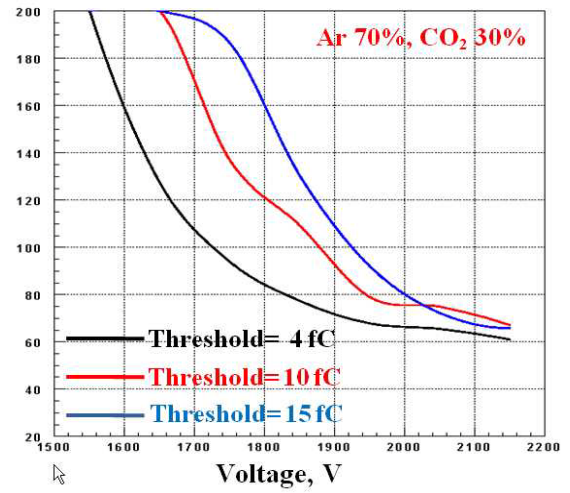
GARFIELD was used to model a single straw tube (2). The gas mixtures were CO<sub>2</sub> 90%, iC<sub>4</sub>H<sub>10</sub> 5%, CF<sub>4</sub> 5% (slow gas) and Ar 70%, CO<sub>2</sub> 30% (fast gas). The dependences of the gas gain on high voltage are shown in Figure 3.

The dependences of spatial resolution and efficiency on the high voltage and thresholds are shown in Figure 4. The threshold for the accumulated charge from the anode wire was set to 4 fC, 10 fC, 15 fC and the resolution was calculated for a distance to the straw wire of 3 mm. The working points (high voltage) were defined on the basis of two criteria; the spatial resolution has not to exceed 40 μm for the gas mixture CO<sub>2</sub> 90%, iC<sub>4</sub>H<sub>10</sub> 5%, CF<sub>4</sub> 5% and 80 μm for the gas mixture Ar 70%, CO<sub>2</sub> 30% and the straw efficiency should not be less than 99% for both gas mixtures. For the slow gas mixture, the working point is 2300 V for the threshold of 4 fC, 2400 V for 10 fC and 2500 V for 15 fC. For the fast gas mixture, it was 1850 V for 4 fC, 1950 V for 10 fC and 2050 V for 15 fC. The dependences of the spatial resolution and the efficiency on the distance to the wire for both gas mixture and threshold 4 fC are shown in Figure 5. The resolutions and efficiencies almost do not depend on the thresholds, if the corresponding optimum working points are used. The r-t dependency is simulated and shown in Figure 6.

Resolution,  $\mu\text{m}$

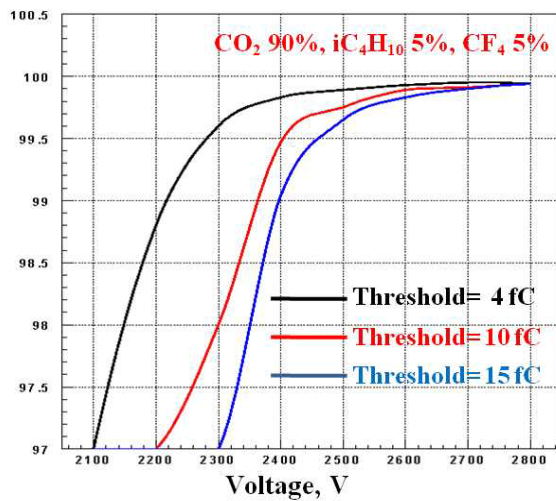


Resolution,  $\mu\text{m}$

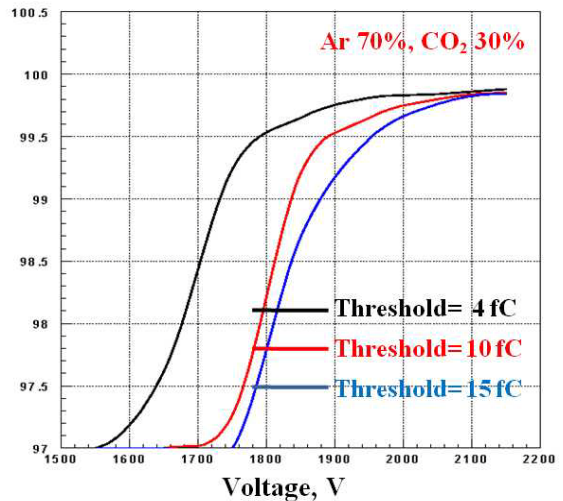


a)

Efficiency, %



Efficiency, %



b)

Figure 4. The dependence of the spatial resolution (a) and the straw efficiency (b) on the high voltage and on the threshold for the gas mixtures CO<sub>2</sub> 90%, iC<sub>4</sub>H<sub>10</sub> 5%, CF<sub>4</sub> 5% and Ar 70%, CO<sub>2</sub> 30%. The spatial resolution was calculated for a distance to the straw wire of 3 mm.

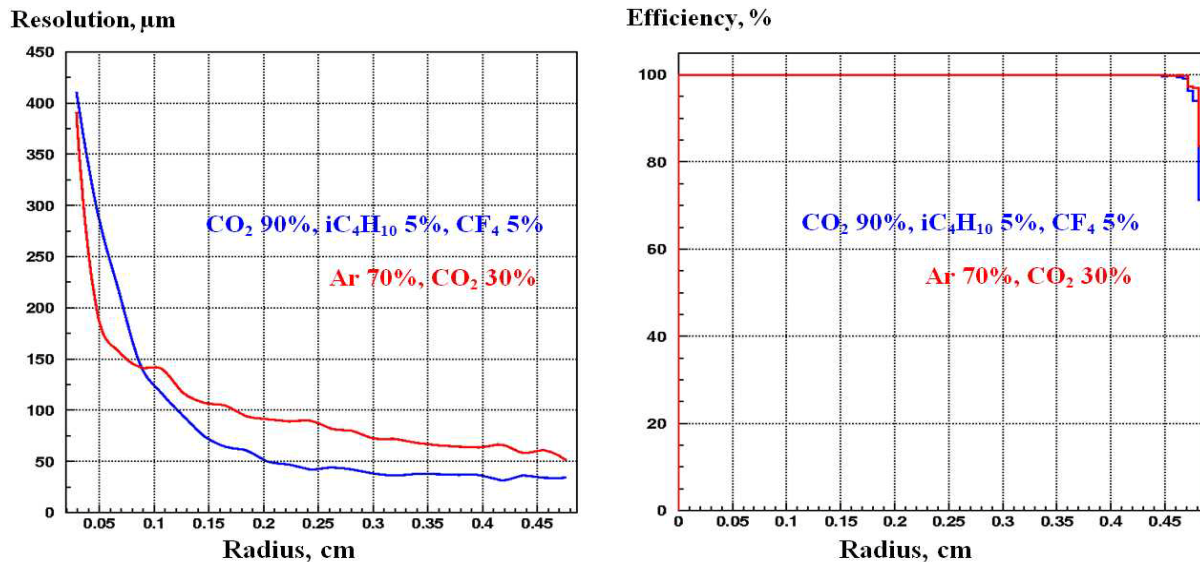


Figure 5. The dependence of the spatial resolution and the straw efficiency on the distance to the wire for gas mixtures  $\text{CO}_2$  90%,  $\text{iC}_4\text{H}_{10}$  5%,  $\text{CF}_4$  5% and Ar 70%,  $\text{CO}_2$  30%.

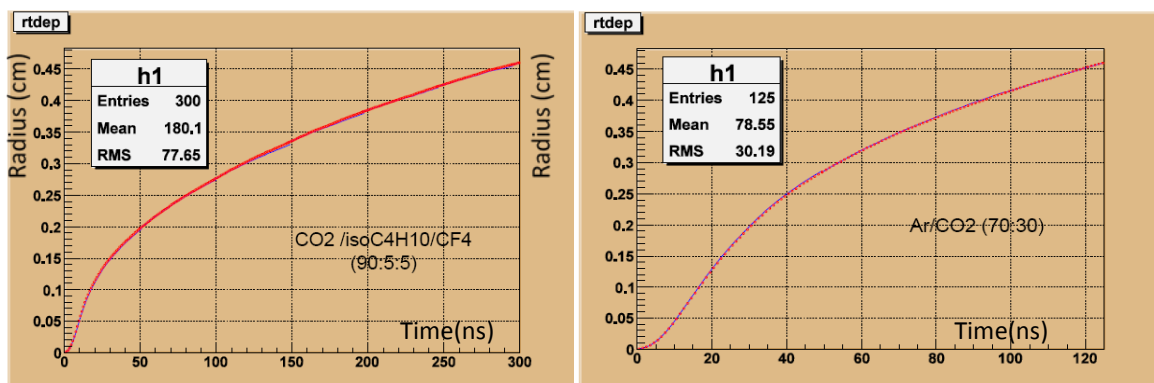


Figure 6. The  $r$ - $t$  dependency for slow (left) and fast gas (right).

### 1.1.1.3 Conclusions from 48-Straw Prototype

To check experimentally the straw resolution and efficiency, a 48-straw prototype was designed and built. The 48 straws were arranged in 8 columns and 6 rows. This prototype has been successfully tested at CERN test beams in 2007, 2008 and 2009 runs with muon and pion beams. A dependency of residuals (that approximately represent the resolution) from track-wire distance for the gas mixture, was obtained in 2009 test run in muon beam as shown in Figure 7 and is qualitatively in agreement with the results from simulations (3).

Ar/CO2(70:30)

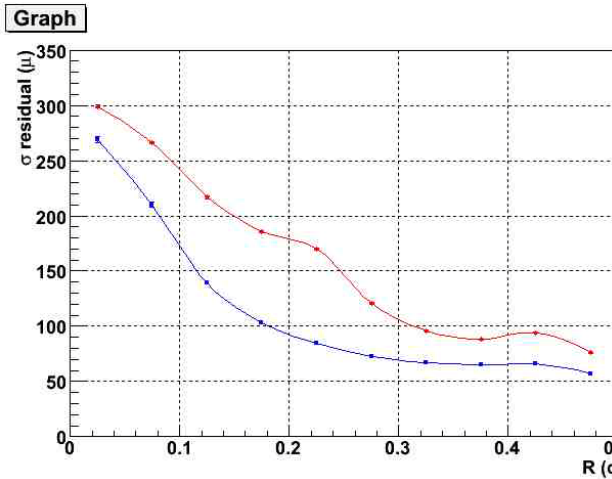


Figure 7. Dependences of the residuals from track-wire distance.

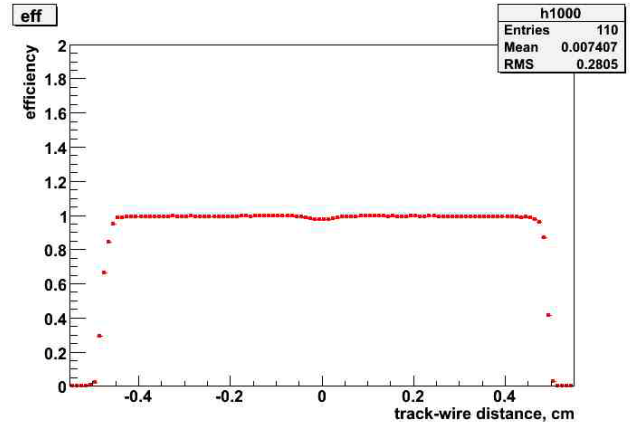


Figure 8. The measured of the efficiency in a single straw as function of the distance between track and wire.

The dependence of the efficiency for a single straw as a function of track-wire distance has been investigated in a pion beam using a CO<sub>2</sub>/isoC<sub>4</sub>H<sub>10</sub>/CF<sub>4</sub> gas mixture. Due to the drop of the straw efficiency near the straw wall, the experimental resolution of the coordinate measurement affects the efficiency. The efficiency drop is smoother than in the results from the simulation, which makes difficult to measure precisely the effective straw radius. Nevertheless, the experimental results confirm the simulation and at the 50% level, the radius (almost unchanged by the coordinate smearing) corresponds to the same radius as in simulation (close to the value of the straw physical radius). The result from measurements is shown in Figure 8.

The dependence of straw efficiency in the straw center on the beam intensity has been investigated in pion beam, using CO<sub>2</sub>/isoC<sub>4</sub>H<sub>10</sub>/CF<sub>4</sub> gas mixture. The result is shown in Figure 9. The efficiency is changed from 99.5 % at 4 kHz down to 97.4 % at 520 kHz. The exact reason for this drop in the efficiency is under study.

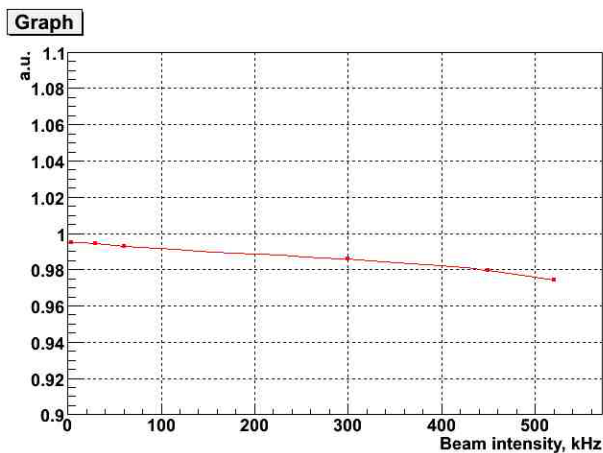


Figure 9. Straw efficiency versus particle rate in a straw.

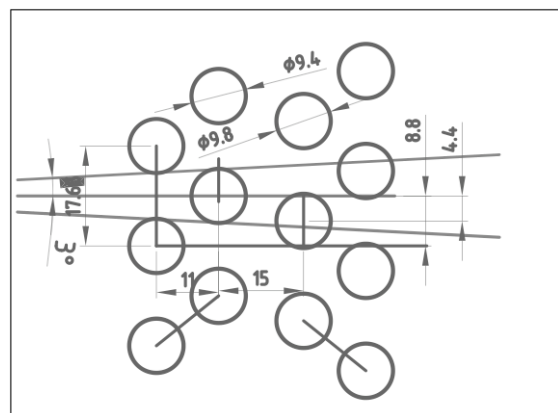


Figure 10. Straw layout in one view (beam direction from left to right). The distance between the straws in one layer is 17.6mm.



### 1.1.1.4 Straw Chamber Layout

The straw layout in a section of one view is shown in Figure 10, to solve the right-left ambiguity, each view has four layers. There are 112 straws in each layer and the distance between the straws in one layer is 17.6 mm. It is enough to guarantee at least two hits per view and be efficient for track angles from -3 to 3 degrees.

### 1.1.2 Wire Centering and Wire Off-Set

Due to the length of the straw and the high voltage on the wire, a calculation of the effect from the electrostatic forces on the wire offset was carried out. The wire offset was calculated using the formula:

$$y = \frac{C}{k^2} \left( \frac{1}{\cos(kL/2)} - 1 \right) \quad (1)$$

where C is:

$$C = \rho g \sigma / T \quad (2)$$

and  $k^2$  calculated from the expression:

$$k^2 = 2\pi\epsilon_0 E_0^2(b) / T \quad (3)$$

(4) where

- $\rho$  =: is the density of the wire
- $\sigma$  =: the cross-section of the wire
- $T$  =: is the straw tension
- $E_0$  =: the field at the straw wall
- $L$  =: the length of the straw
- $\epsilon_0$  =: has the value  $8.854 \times 10^{-12}$  As/Vm

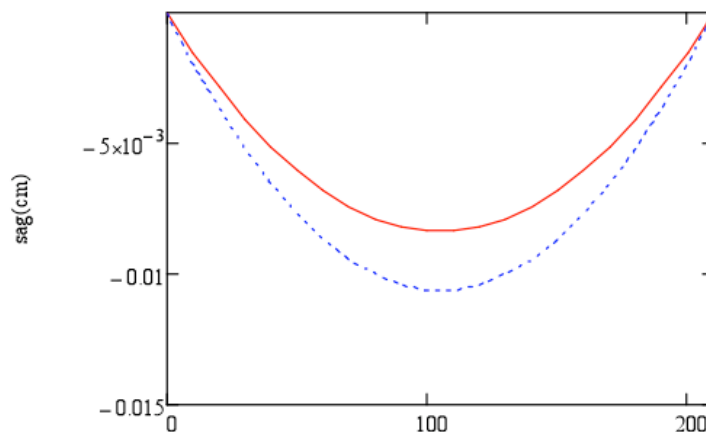


Figure 11. The wire deflection for a 2.1m long straw with (blue) and without (red) electrostatic deflection at 2.5 kV.

The results plotted in Figure 11 shows an amplification of the wire sag of  $\sim 27\%$ , due to the electrostatic forces. The voltage was set to 2.5 kV (slow gas) and the tension in the wire to 90 g. For the fast gas with a high voltage of 1.8 kV, the corresponding increase in the wire sag is 9%.

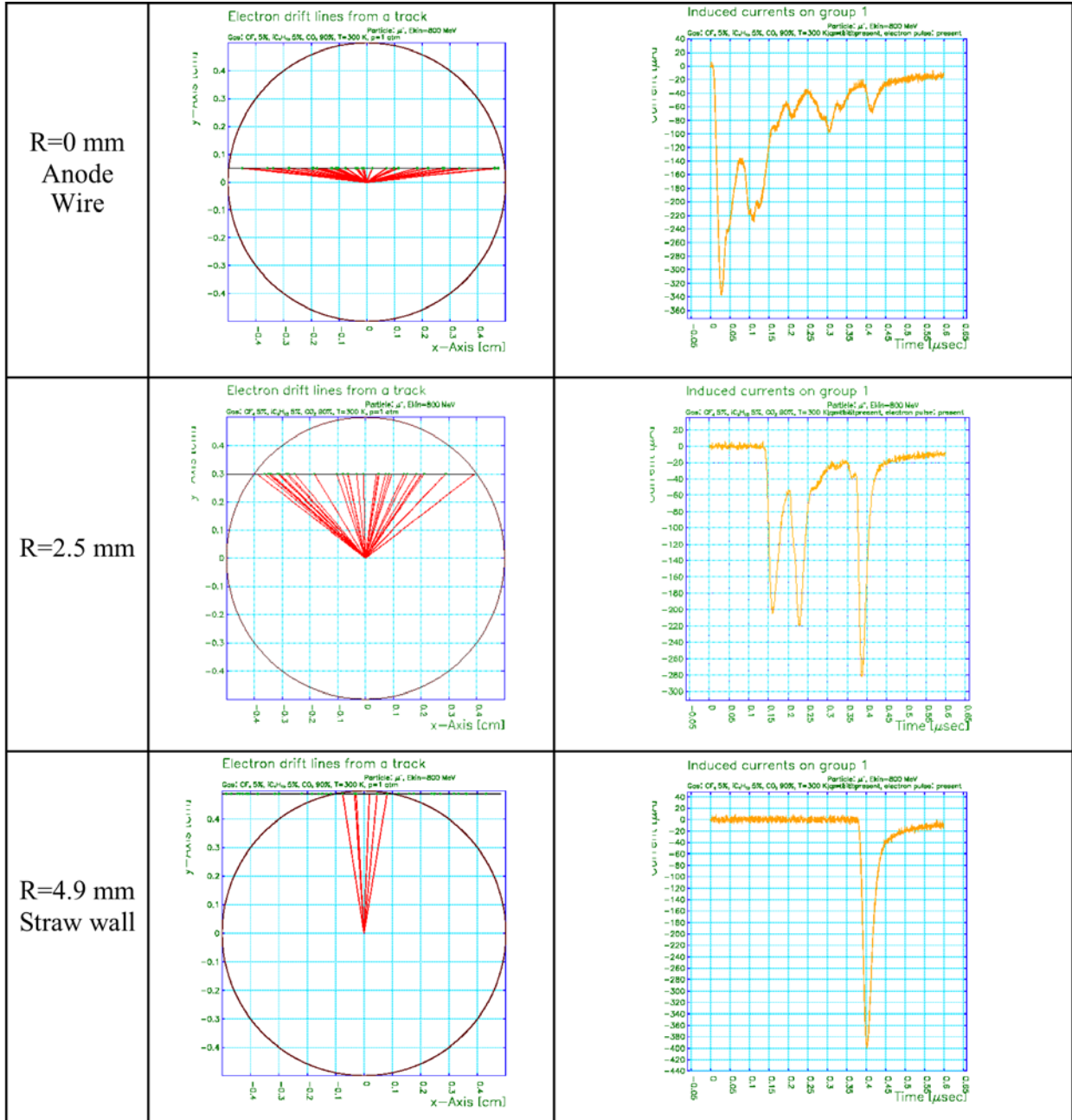


Figure 12. Signal shape for muons for different distances between tracks and straw centre (simulation using Garfield).

### 1.1.2.1 Straw Signal

The straw signal shapes for muons were simulated with Garfield and a few examples are shown in Figure 12. The straw diameter is 10 mm and the anode wire diameter 30  $\mu\text{m}$ . The gas mixture is  $\text{CO}_2/\text{isoC}_4\text{H}_{10}/\text{CF}_4$  (90:5:5) with a gas gain of about  $10^5$ . A track contains a number of clusters with 1-3 primary electrons in each. The average number of clusters for a 1 cm long track is about 75.

The characteristic impedance of a straw as transmission line and as a function of frequency, is calculated using the following formula (see Figure 13).

$$Z_c = \sqrt{\frac{L}{C}}$$

With  $L$  ,  $C$  ,  $G$  = conductance between the straw and the wire ,  $\epsilon$  and  $\mu$  . At high frequencies the impedance can be expressed as

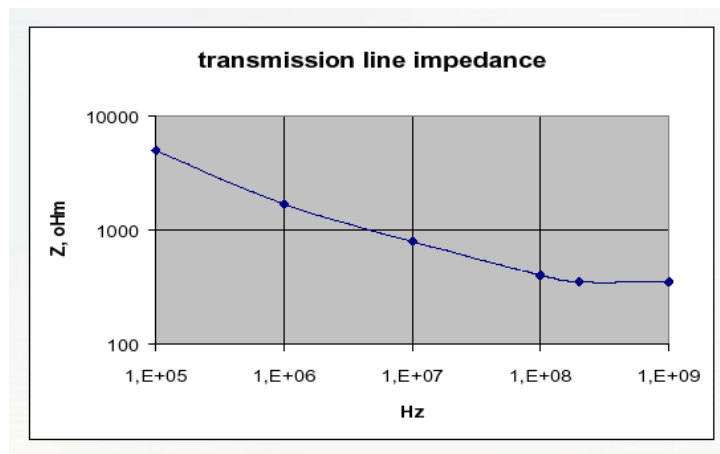


Figure 13. The dependence of the straw impedance from the frequency.

An example of the signal reflection study by the Spice program is shown on Figure 14. The current division and the signal attenuation are clearly visible. The signal reflection phase depends on the value of  $R_1$  and  $R_s+R_{in}$ .

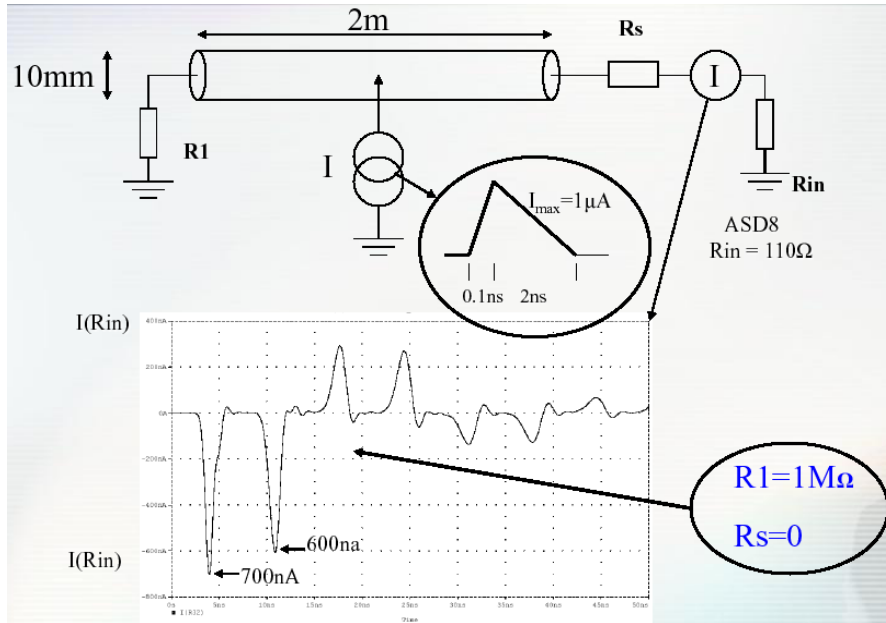


Figure 14. Signal reflection simulation with SPACE.

The result of the signal termination optimization is presented in Figure 15. A resistor R1 of 350 Ω cancels the reflection at the “far” straw end. With  $R_s=0 \Omega$  the signal amplitude is higher by factor 1.5, compared to a termination of 240 Ω.

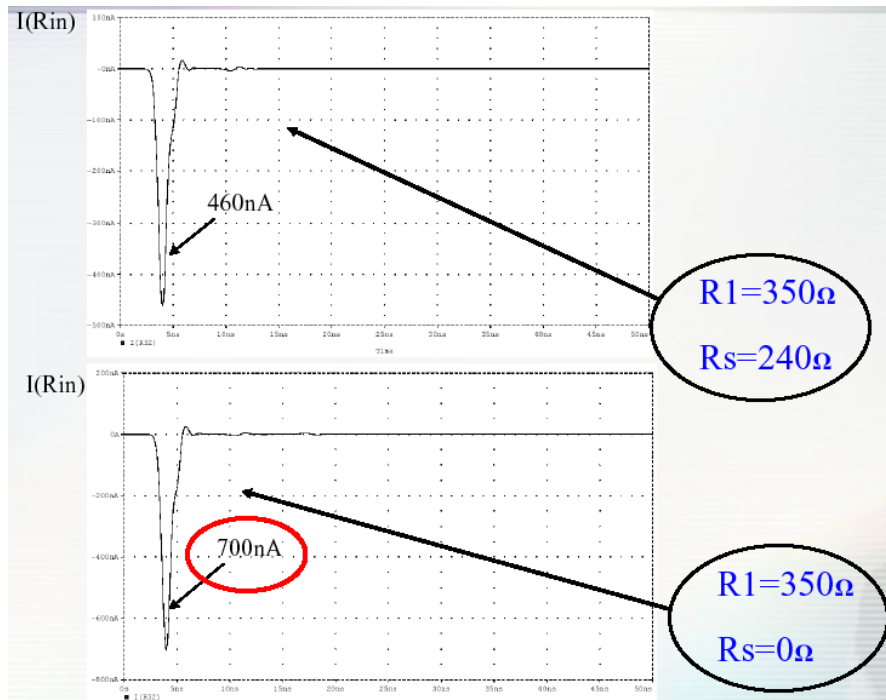


Figure 15. Optimal signal termination for the straw.

The signal reflections in the straw have been studied experimentally. A schematic of the set-up is presented in Figure 16. The straw diameter is about 10 mm, the anode wire diameter 30 μm, the straw length 210 cm, the straw capacitance 20 pF and the straw inductance 2.5 μH. Furthermore, the anode wire resistance is 250 Ω and the cathode resistance ~70 Ω. A fast current

amplifier (rise time about 10 ns) with a gain of 25 mV/ $\mu$ A and input impedance of 120  $\Omega$  was used. The straw termination resistor had the following values: 0  $\Omega$ , 250  $\Omega$  and 1 M $\Omega$ .

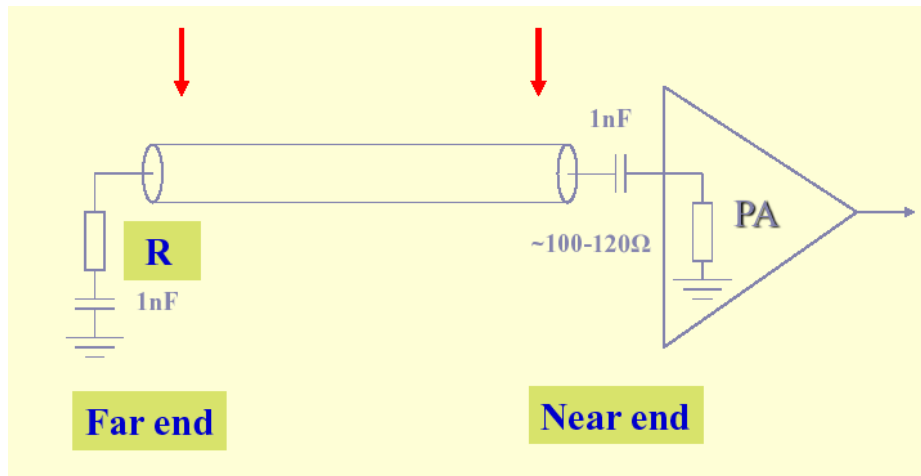


Figure 16. Set-up for straw termination experimental study.

A radioactive source Fe-55 (gamma, E=5.9 Kev) was used. The influence by each option of straw termination on the amplifier signal shape and its value is presented in Figure 17. The optimal straw termination (no signal reflection) is for R=250  $\Omega$  (C blocking=1000 pF). The signal attenuation value from the “far” straw end is about 55%.

The straw acts like a transmission line with the characteristic impedance of 350  $\Omega$  at high frequency. The straw “dead” time increases (reflections are up to 100 ns long) and at high rates, the reflections may deteriorate the signal. Experimentally it was shown that the “far” end should be terminated with a resistance of 250  $\Omega$ , if the capacitance of the blocking capacitor is 1000 pF and at the “near” end, there is no termination resistor ( $R_s=0$   $\Omega$ ). The signal attenuation along the straws is 55%. However removing the signal reflections with the termination also decreases the signal amplitude. The final choice on the straw termination will be done once the data from the 2010 test beam is analyzed (see also 1.1.110).

### 1.1.3 The Straw

The most important constituents of this detector are 7'168 Straws. Each straw is the cathode of a drift tube that is capable to operate inside vacuum. A straw tube is manufactured from thin polyethylene terephthalate (PET) foil that is longitudinal welded (ultra-sonic weld) to form a tube. The straw has an active length of 2.1m long and a nominal diameter of 9.8mm<sup>2</sup>. It's inner surface has a metal coating (Cu/Au) to provide electrical conductance on the cathode.

<sup>2</sup> The exact diameter of the straw depends on its overpressure. 9.8 mm corresponds to the diameter without any overpressure (manufacturing conditions).

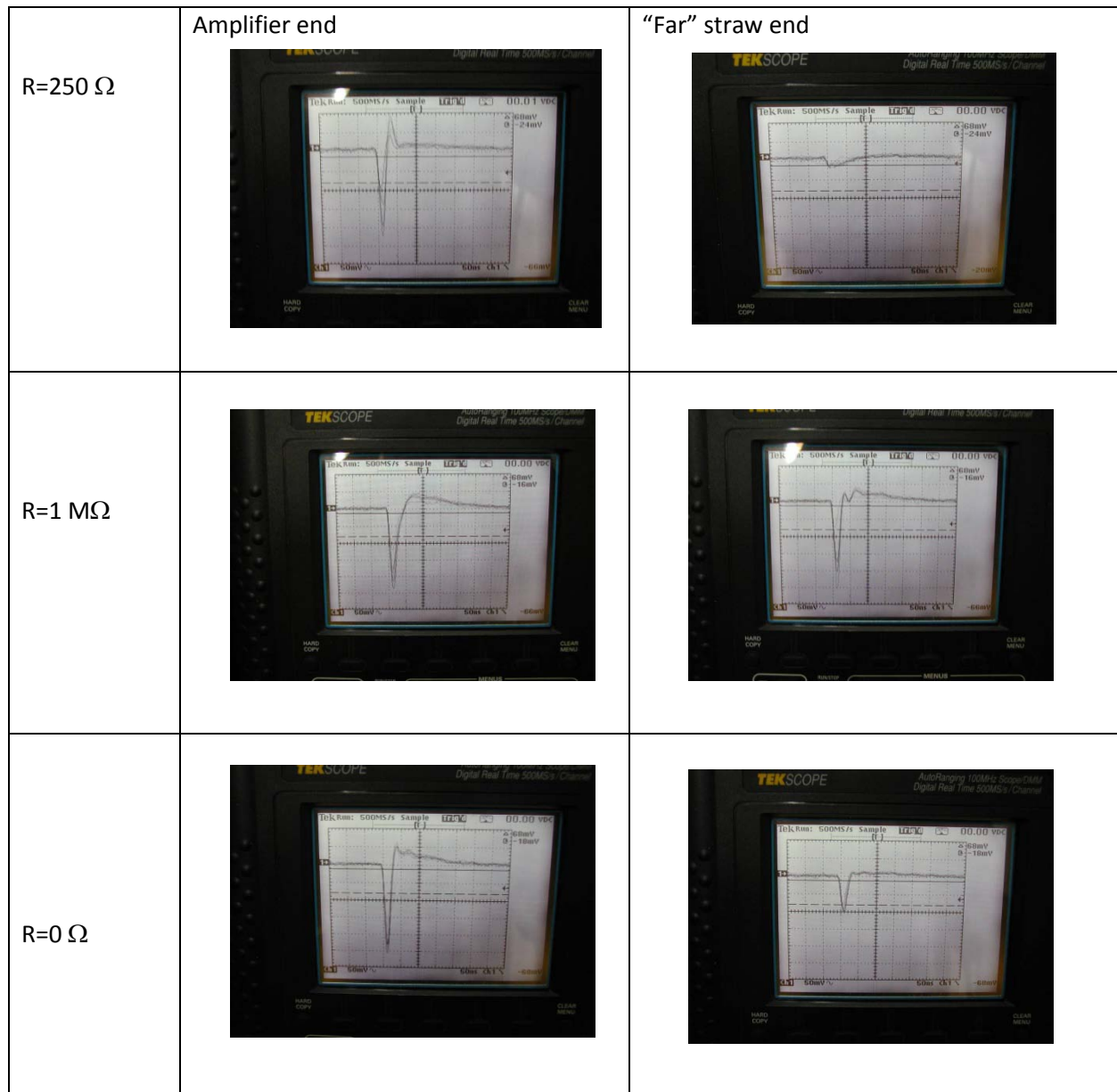


Figure 17. The signal shape for different straw terminations.

### 1.1.3.1 Material

The choice of the straw material is a compromise between many different requirements, i.e. radiation length, permeation of gases, mechanical properties, adhesion to metal coating, bonding with epoxy and the ability to be ultrasonically welded into a tube. A summary of the specifications is given in Table 2.

Table 2 Summary of coated material specifications

Description	Specifications
PET film	polyethylene terephthalate type Hostaphan RNK 2600 of (36 ± 2.0) μm thickness
Density	1.4 g/cm <sup>3</sup>
Copper layer thickness	50 nm
Gold layer thickness	20 nm
Resistivity of finished straw (2.1m)	~70 Ω
Permeation of naked film (10 <sup>-12</sup> Torr·l·cm/s·cm <sup>2</sup> ·Torr)	6 for He, 0.06 for Ar, 1 for CO <sub>2</sub>

The straw tubes for the tracking detector in the NA62 experiment are manufactured from a biaxially oriented coextruded film made of polyethylene terephthalate (PET). One side of the film is chemically pre-treated to improve adhesion; this side was chosen for the epoxy bonding between the straw tube and the (PEI) polyetherimide straw fixation plug. The thickness of the film is 36 μm, and the non-treated side is coated by a conductive layer of 50 nm of Copper (Cu) followed by a protective layer of 20 nm of gold (Au). Once the tube is manufactured, the conductive layer, is found on the inner diameter of the tube, while the outer diameter remains uncoated, but chemically pre-treated for gluing.

### 1.1.3.2 Long Term Tests

Long-term tests were carried out with straws mounted under tension with a load of 15N applied before the extremities of the tubes are bonded to the PEI supporting parts. The sag and the tension of the tubes were measured during a long-term test (18 months). Values are recorded with straws under pressure (in order to simulate the final experimental set-up conditions in vacuum) and compared to a reference straw at atmospheric pressure.

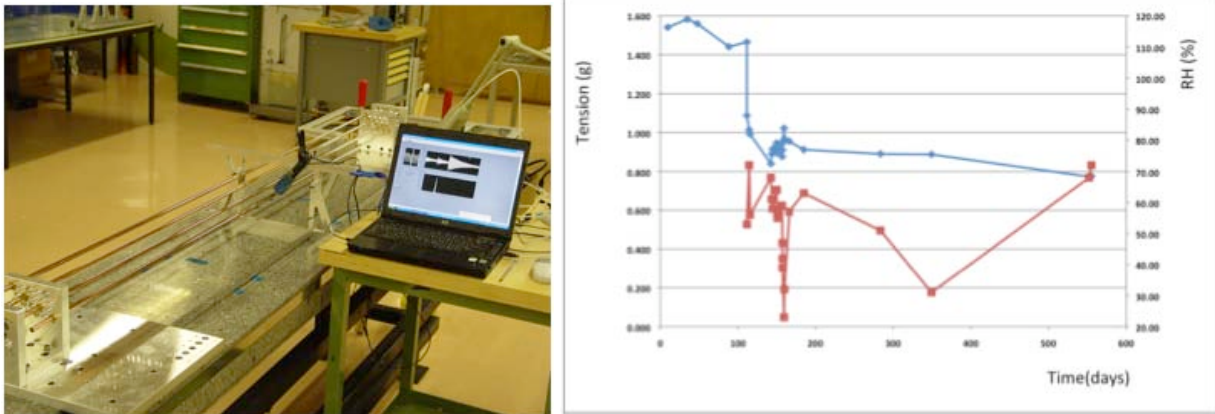


Figure 18. A view of the long-term test apparatus (left) and the straw tension (blue curve) over time. The red curve indicates the relative humidity.

### 1.1.3.3 Tensile Test of PET samples:

The base material for the straw tubes was tested on CERN’s Instron tensile test apparatus. The values observed for welded samples are typically 25 % lower than those of the coated un-welded PET. Un-welded PET has a tensile strength close to 130 MPa whereas welded and coated samples fail at ~100 MPa. The stress in the straws due to the pressure difference (~1 bar) is 13 MPa which gives sufficient safety margin.

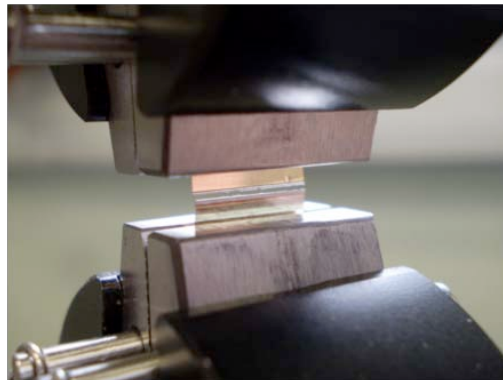


Figure 19. Close-up view of a tested sample (the weld in the center).

### 1.1.3.4 Coatings and Permeation:

The metal coatings are accomplished by a sputtering process; the metallisation provides electrical conductivity as well as an improvement in the permeation properties of the PET substrate. Measured values of permeation through a 50 nm Cu coated membrane show a BIF (barrier improvement factor) of 8.5 for He (helium); 9 for CO<sub>2</sub> (carbon dioxide) and 5 for Ar (argon). The quality of the sputtered coating is measured by a peel test using adhesive tape.

### 1.1.3.5 Scanning Electron Microscope Investigations

The coated PET was observed using scanning electron microscope (SEM); this showed the quality of the coating and sputtering on the substrate. The SEM was also used to verify the metal coating thickness, not as a direct measurement, but by using the EDX (energy-dispersive x-ray spectroscopy) facility and a third party software.



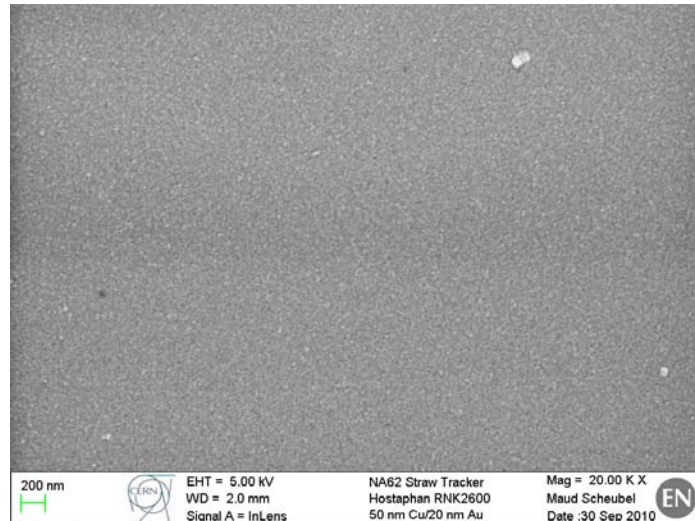


Figure 20. A typical view of coated PET with a magnification of 20 000 (RNK 2600).

Metal coating and weld quality of the seam was checked using both SEM and traditional optical microscopy (see Figure 20 and Figure 21)

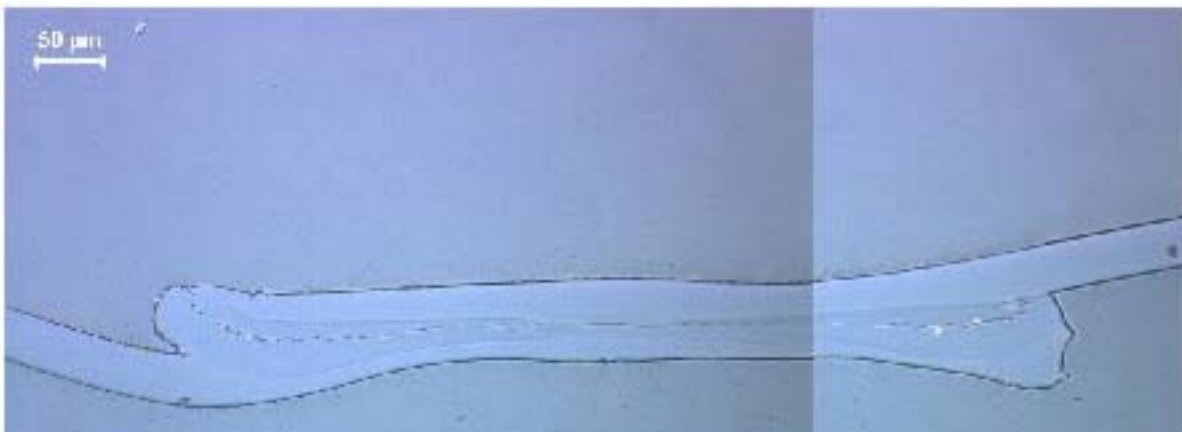


Figure 21. Cross section of a welded seam where the two sides of the strips are fused.

### 1.1.3.6 Glue Bonding Test

The adhesion between the outer diameter of the straw tube and the PEI straw support is critical. The selected epoxy resin for this operation was TRA-CON's TraBond 2115 whose out gassing properties and radiation hardness were studied at CERN. This epoxy has a good resistance to shocks and temperature cycling. Its pot life is close to two hours and curing in 24 hours. Samples of PET were peel tested after being bonded to an aluminium plate. The bond of the selected candidate was greater than the natural resistance of the material. The selected material was also analysed by X-ray photoelectron spectroscopy. This allowed us to better understand the chemical treatment made by the PET suppliers and its effects on bonding.

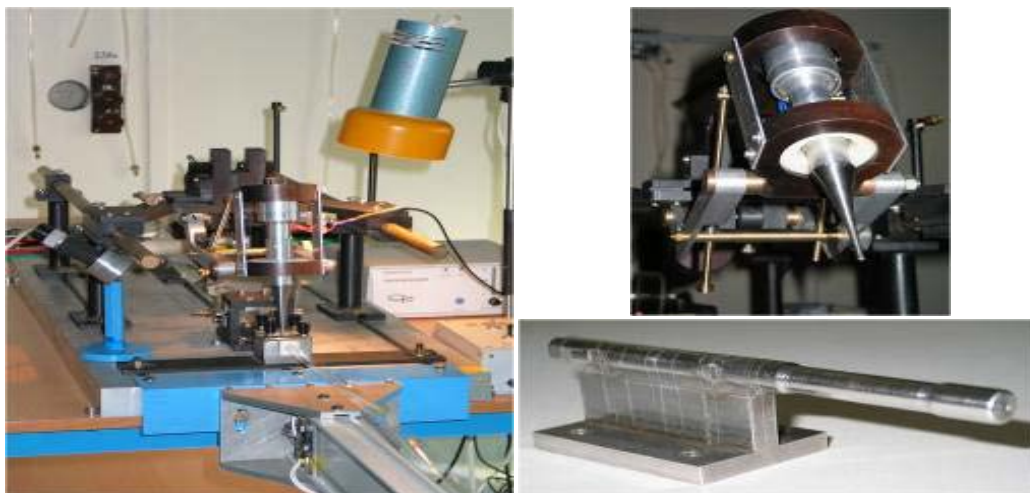


Figure 22. A new machine for straw production (left), new ultrasound head (right top) and anvil (right bottom).

### 1.1.3.7 Straw Manufacturing and Welding

A dedicated machine for straw production has been designed and constructed to manufacture the 7168 straws (see Figure 22, left). An ultrasound head with movable fixation at the frame (the Figure 22, right top) and anvil for straw welding (see Figure 22, right bottom) were designed and constructed to obtain a good quality of weld seam (see Figure 23) and to minimize differences in straw diameter. The distribution of the straw seams widths and tube diameters obtained during the production of a large set of straws are shown in Figure 24 and Figure 25. After manufacturing, each straw is equipped with glued end plugs and leak tested. All measurements are individually recorded in a logbook where all straw characteristics are stored like material, manufacturing date, inner diameter, etc. A unique serial number is allocated to every straw tube and a complete feedback is readable at any moment of the detector assembly.



Figure 23. Quality of the weld seams (0.4 mm – left picture, 0.85 mm – right picture); 60 times magnification.

### 1.1.3.8 Straw Conditioning

Once the ultrasonic welding apparatus produces the straws, they need to be carefully stored, prior to installation into the detector. The straws need to be stored during a period of time that varies from several weeks to several months. The tube storage has several constraints that need to be addressed:

The inner diameter of the tube must remain free of dust, and of foreign particles.

The tube must also have the ability to be manipulated by technicians without buckling.

With the above constraints in mind, it was decided that the optimal way to store the tubes would be under pressure. This would also have the added value that the changes of pressure in a tube with respect to time could be observed. Straws that show gas leakage and have poor weld quality can be removed. Taking into account further quality control tests that are performed on the tubes before installation, and the manipulation of the tube itself during its installation into the detector, a dedicated system was developed, in the form of valves as shown in Figure 26.

For storage, the straws are gas filled with an approximate overpressure of 1 bar. The loss of pressure over time is measured indirectly by measuring the local straw deformation under a 300g weight and comparing with the day it was first pressurized. The first valve must have the ability to let gas into the straw, then act as a non-return valve, thus keeping the straw under pressure. The valve design is loosely based on the “Dunlop” / “Woods” valve design, with an additional feature. To prevent leakage through the non-return system, an O ring and threaded screw have been added. This is also used to fit the gas connector.

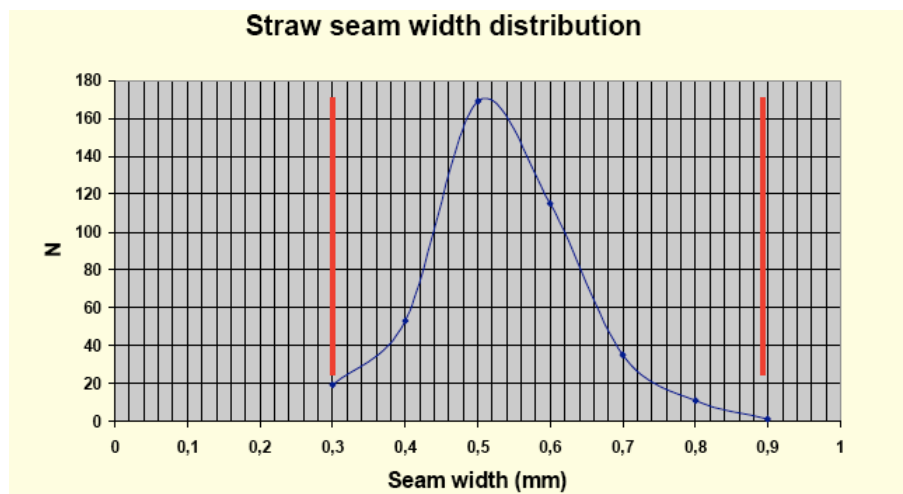


Figure 24. Weld seam widths distribution.

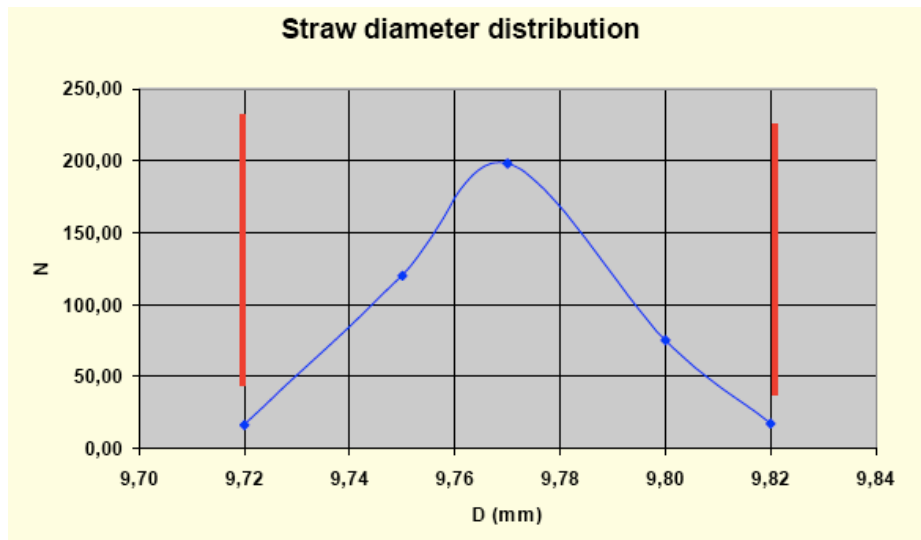
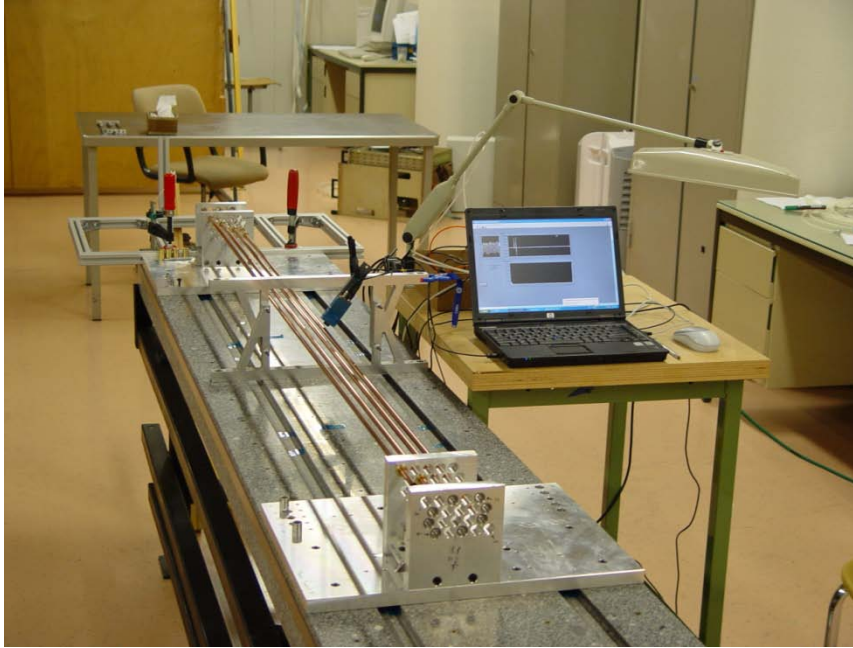


Figure 25. Straw diameters distribution



Figure 26: The PEI non-return valve (left) and the opposite side with O ring and an M4 screw.

The second valve, used on the other extremity of the straw tube, it is a simplified version without the non-return mechanism. To run a leak test, we simply connect the test system to an M4 thread inside the valve and pressurise the straw. To simplify Sagitta measurements of the simply supported tube both valves are of the same weight. In addition, the ends have the ability to be connected to standard M4 threads. Furthermore, both valves have an outer diameter smaller than the straw tube outer diameter, which allow the straw tube to be installed under pressure. This facilitates the manipulation of the straws and limits the risk of buckling the straw wall and the welding seam.



*Figure 27. Set-up to measure the straw sag and frequency as a function of different pre-tension and pressure. The computer is connected to an IR emitter and receiver (OPB732) to measure the frequency of the vibrating straw.*

### 1.1.3.9 Mechanical Properties and Pre-Tension of the Straw

#### 1.1.3.9.1 The Measurement of the Straw- Sag

In order to determine the necessary straw pretension, a dedicated set-up was designed to measure the straw sag and the straw frequency, as a function of pressure (see Figure 27). In order to simulate the effect of the vacuum, the straw was connected to a gas bottle and the absolute pressure inside the straws was set to 2 bar. Four straws were glued horizontally into two plates. One straw was equipped with a sliding fixation on one end to allow for variable straw pre-tension. However, the sliding end of the straw was blocked (clamped ends) before measuring the deformation (sag) and frequency. The results are shown in Figure 28. The increase of the sag, as the pressure inside the straws increases, is clearly shown.

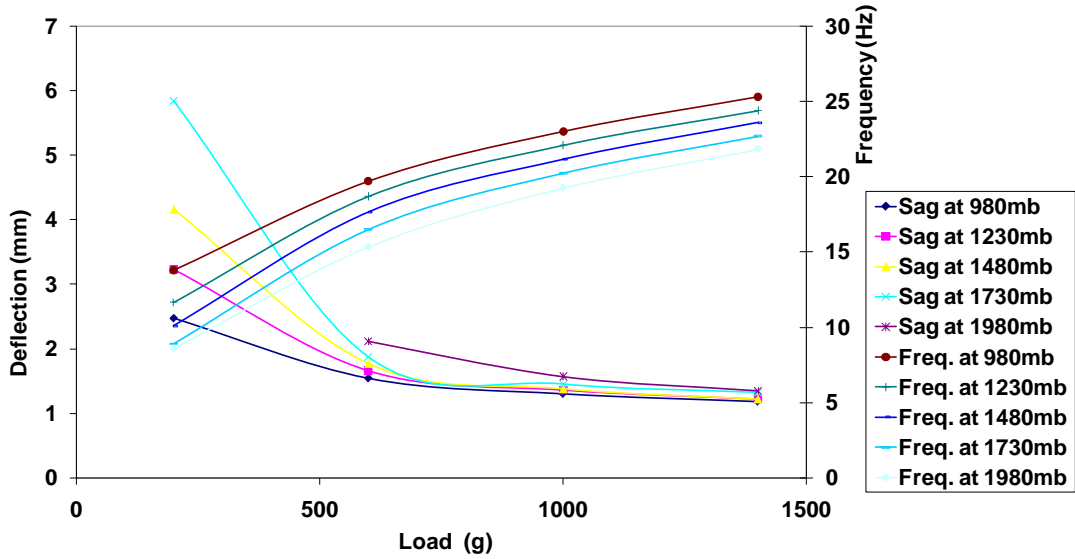


Figure 28. Measured sag and frequency of the straw as function of pre-tension at different over pressures.

### 1.1.3.9.2 Pressure Influence

A study of the straw sag as function of overpressure at different pre-tension was carried out to determine the required straw tension. The results are shown in Figure 29. A minimum tension of 10N is necessary to obtain an acceptable straw straightness. We have decided to apply a force of 15N during installation in order to allow for some loss of tension over time (5).

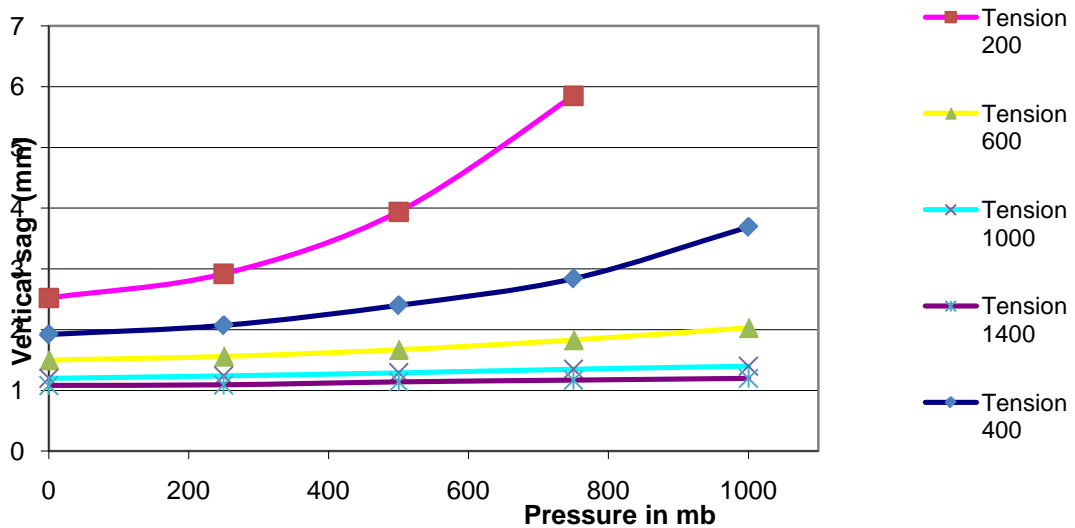


Figure 29. Straightness as function of pressure for a 1.85 m long horizontal straw for different values on the pre-tension (g).

## 1.1.4 Chamber Design, Construction and Installation

### 1.1.4.1 Detector Geometry and Layout

The detector consists of four stations and each station has four views and gives four measuring points  $(x,y,u,v)$  as shown in Figure 30. The mechanical structure of the chambers requires good dimensional stability, rigidity and strength. The active volume of the detector is 2.1 m x 2.1 m and each straw plane has a 12 cm wide region for the beam in the middle of the frame without straws. A 3D drawing of a chamber is shown in Figure 31.

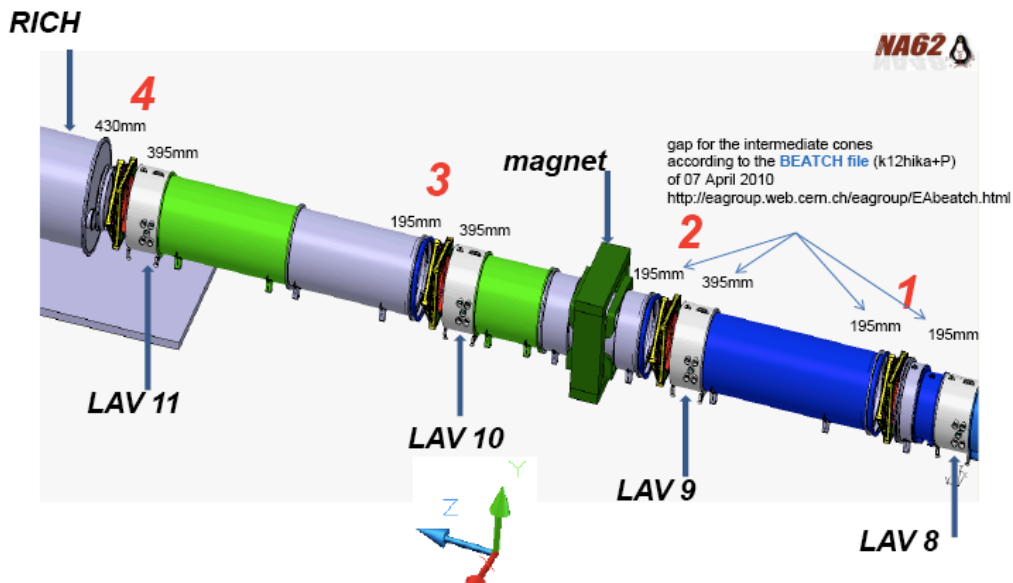


Figure 30. Layout of the straw spectrometer in ECN3 with the straw chambers marked 1,2,3 and 4.

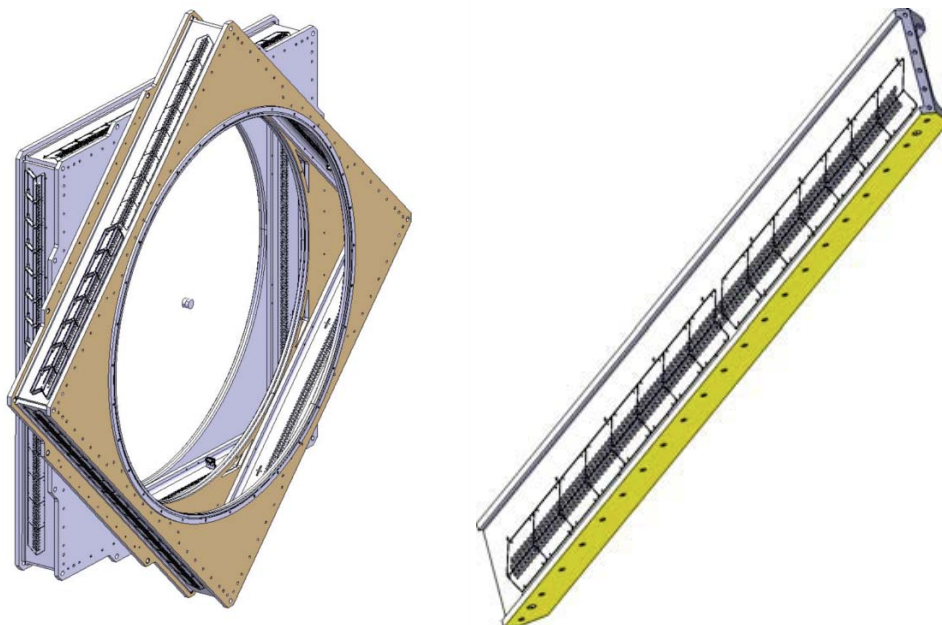


Figure 31. One chamber consisting of two modules (left). Detail of the straw fixation beam (right).

The chambers consist of two modules and each module is built from six parts; four beams for the fixation of the straws and two flanges. The basic element during the detector assembly and testing is the module.

### 1.1.4.2 Mechanical Validation of the Design

In order to dimension the mechanical structure of the detector, a finite element model (FEM) of the chamber and of the interface parts (between chamber and vacuum tube) was built. The aim is to calculate the deformation of the chambers and to verify that the stress levels are acceptable in the different parts. In addition, the model is used to determine the dimensions of the fixation bolts.

The following loads have been applied to the chambers and interface parts for the calculations:

- A straw tension of 14.7 N/straw
- A pressure difference of 1 bar between the outside and the inside (straw volume) of the chamber
- An axial force of 30 t on the interface parts, originating from the atmospheric pressure pushing on the end cap of the decay tube (a plate of ~ 2m in diameter)
- The gravitation
- Note: The wire tension of 0.9N/wire was neglected.

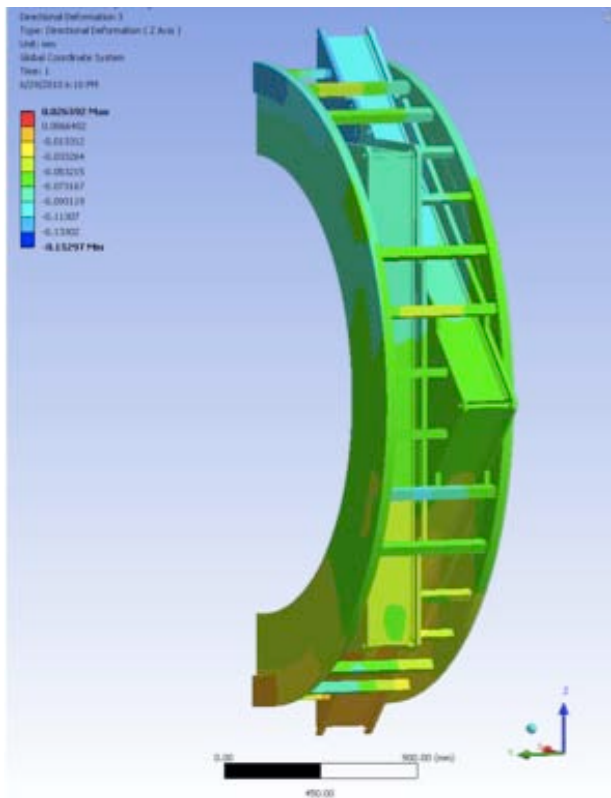


Figure 32. Calculation of the chamber deformation.

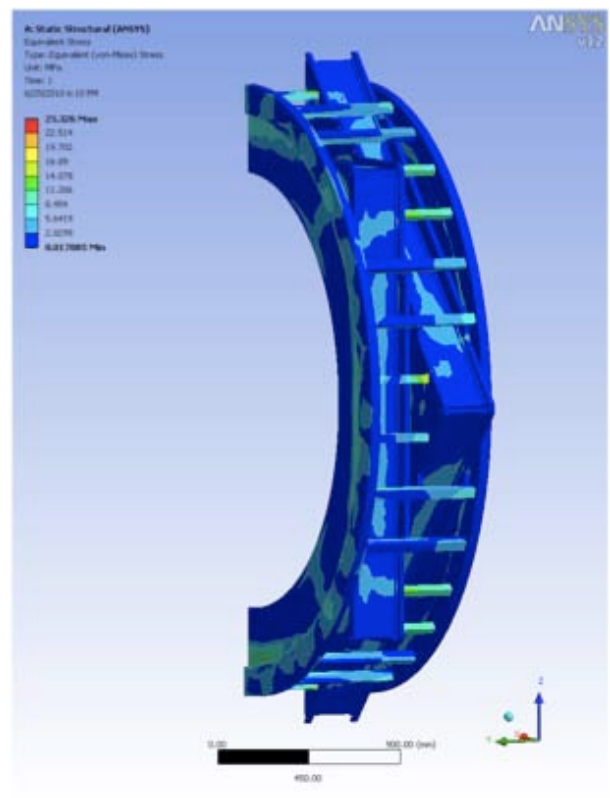


Figure 33. Calculation of the equivalent stress levels.

The resulting deformations and the stress levels are shown Figure 32 and Figure 33. The maximum deformation is 0.2mm and the highest stress level is calculated to < 10 MPa. For comparison it can be



mentioned that the elastic limit is around 145 MPa. In this context it should be pointed out that some safety was privileged at the cost of a somewhat higher weight. The total weight of a chamber is 1200kg (2x 600 kg).

#### 1.1.4.3 Structure Assembly and Tightness

One of the challenges in the NA62 tracker construction is the structure gas tightness. The chamber will be built using four “H” beams linked to two octagonal flanges, as shown above in 1.1.4.1 The whole chamber will be bolted together and then sealed by a two-component epoxy resin in the joining surfaces. A prototype of the corner was built in order to validate the assembly technique (see Figure 34).



Figure 34. Prototype detector's inner corner (left) and a set-up verify leak tightness (right).

### 1.1.5 Detector Components and Assembly Principles

#### 1.1.5.1.1 Active Web and Wire Connection

A cross-section of the mechanical structure holding the straws is shown in Figure 35. An Aluminum frame has precisely drilled holes for precise positioning of the straws and wires. The modularity in terms HV, gas supply and readout is 16 straws. Removable partitions for the gas manifold and a dedicated polyurethane joint for gas tightness was developed. The partitions also serve as supports for the so-called cover, which contains the front-end electronics (FE), high-voltage and gas connections. Between the straws and the frame are glued insulating sockets in polyetherimide (PEI) (see Figure 36).

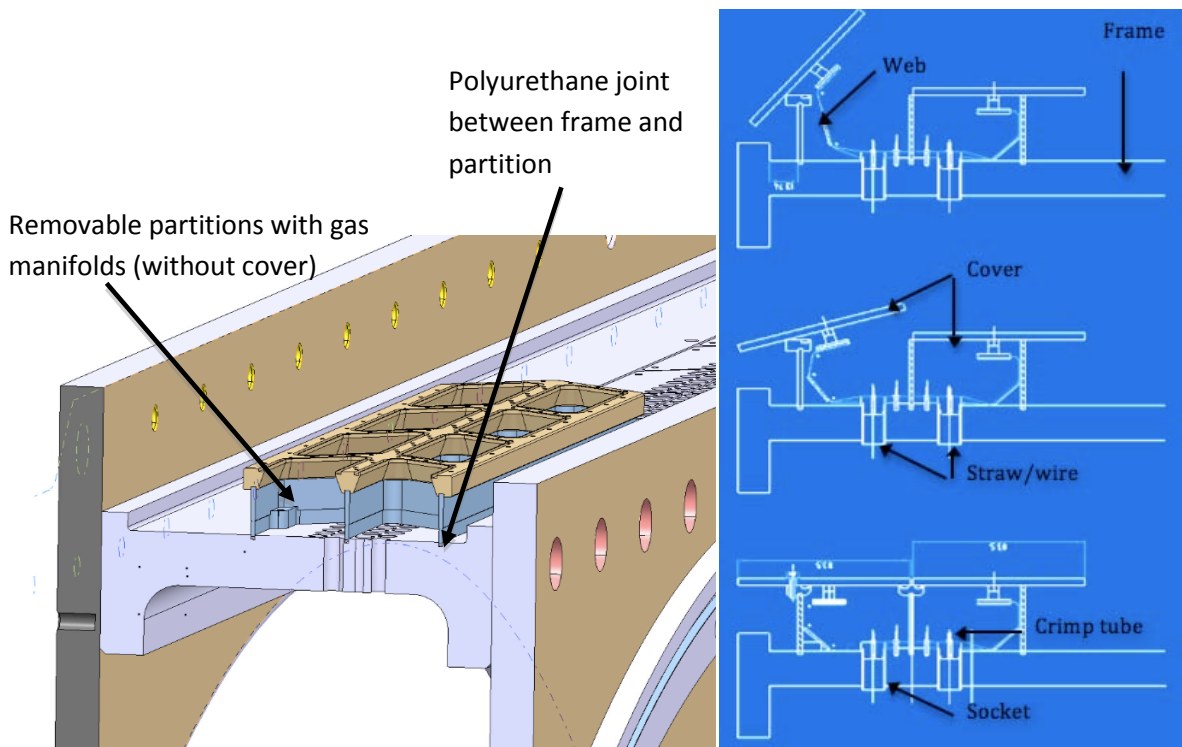


Figure 35 Principle cross-section showing detector frame with gas manifold and cover (left). A schematic view showing how the web connects to the straws and wires to the inside of the cover (right).

One of the key components of the chamber is the so-called active web, shown in Figure 37. The active web is a multi-layer flex-rigid printed circuit board, which carries the high voltage to the wire and transmits the signal back to the front-end electronics. The web has two connectors; one for HV and one for the signals. The web connects to the backside of the cover, which is shown in Figure 38. The cover does not only provide the leak tightness of the manifold, it also comprises the front-end electronics, high voltage and gas connections. The front-end chip is the 8-channel CARIOCA chip which was developed for LHCb (6), (7) .



Figure 36. Details of the straw end-pieces are shown. The socket is glued between the straw and the structure (left). The connection plug pushes the petals of the web to the straw wall. The crimp-tubes connect the wire to the Kapton® layer of the web circuit by crimping (left picture) or by soldering (right picture).

The wire is tensioned and positioned using a copper tube inserted in the so-called connection plug (see Figure 36). The copper tube connects to the second layer of the web, which brings the high voltage to the wire and the signal back to the front-end electronics. At present two options for stringing the wires are studied; one based on crimping and one where the wire is soldered to a copper tube (see details in 1.1.11 on page 42).

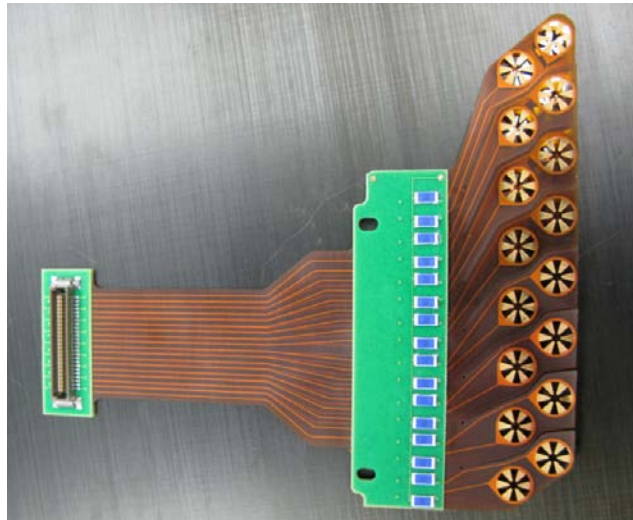


Figure 37. Detail of the flex-rigid circuits board (web) that connects to the straws (ground) and the wire (high voltage and signal).



Figure 38. Front-End board (cover) with the two CARIOCA chips (front side). The cover is mounted on partition serves as a leak-tight roof for the gas manifold and fed through for gas, high-voltage and signal connections to the straws (back side).

#### 1.1.5.1.2 Alignment Tool for the Straw Insertion and Alignment

In order to keep the straws straight the straws are pre-tensioned with a force of 14.7 N. Mechanically, the straw under tension behaves like a string joining the two sides of the mechanical frame. By using spherical bearings, the straw is brought under tension while it is in vertical position (see Figure 39). The spring keeps the pre-tension on the bottom center pin during the gluing process. The pre-tension in combination with the bearings self-aligns the two pins, which hold the straw during the gluing, and

guarantees the straw straightness. Using a digital microscope fixed on a linear rail we measured the straw straightness under a tension. The measured straightness was better than  $100\mu$ . This measurement validated the assembly principle. The influence of gravity on a 10 N tensioned straw, tilted at  $45^\circ$ , was measured and showed a deformation of  $\sim 300\mu$ . This sag is too large for safe operation and imposed a spacer support development (see 1.1.5.1.3).

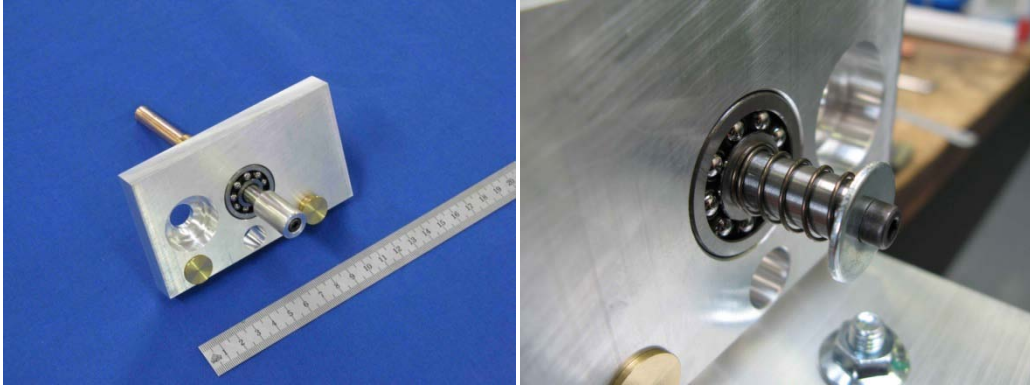


Figure 39. Alignment support with spherical bearings and (left) and the spring-loaded tension tool (right).

### 1.1.5.1.3 The Spacer

In order to support a straw along its length each straw is held by two “spacers” (see Figure 41). In this configuration the maximum unsupported straw length is  $\approx 70$  cm . In order to minimize the amount of material, the spacers consist of polyetherimide (PEI) rings surrounding the straw ( $\Phi_{\text{inner}} = 9.92$  mm,  $\Phi_{\text{outer}} = 10.40$ mm,  $H = 3$ mm). The weight of one ring is 0.018g. They are glued at a distance of 17.6 mm from each other between two CuBe wires with a diameter of 0.1mm. The wires are given a tension of 500g to guarantee the straightness at all times. A shorter version of the spacer for the 64-straw prototype (see Figure 50) is shown in Figure 40.

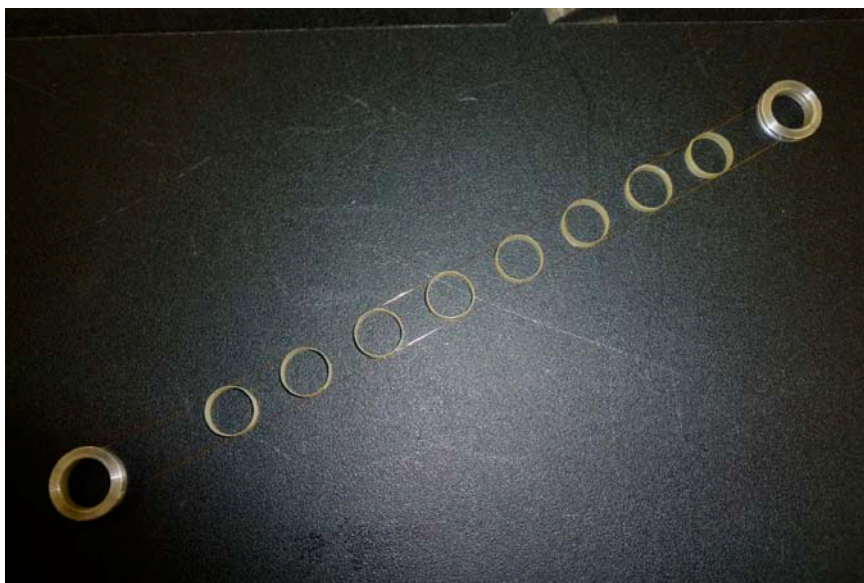


Figure 40: The spacer made for eight straws with a metal ring for alignment and tensioning at both ends. The PEI rings are seen in the center.

The design and assembly procedure was validated in a full-length prototype and measurements showed a maximum difference between the measured and theoretical ring position (ring centre) of 10  $\mu\text{m}$  along the 2 m long spacer.

#### 1.1.5.1.4 Straw Tension Measurement

Straw tension is measured with a long distance infrared reflective switch (OPB732). It measures the frequency of the straw vibration. The output of the device is connected to the microphone input of a laptop equipped with a LabVIEW® program. It displays the natural frequency of the straw and calculates the straw tension. The principle is similar to the wire tension measurement except a smooth rod is used to excite the straw instead of a current pulse in a magnetic field as in case of the wires. A schematic view of the set-up and the LabVIEW® panel is shown in Figure 41. Note the straw spacers limit the movement of the straws and create two nodes along the straws.

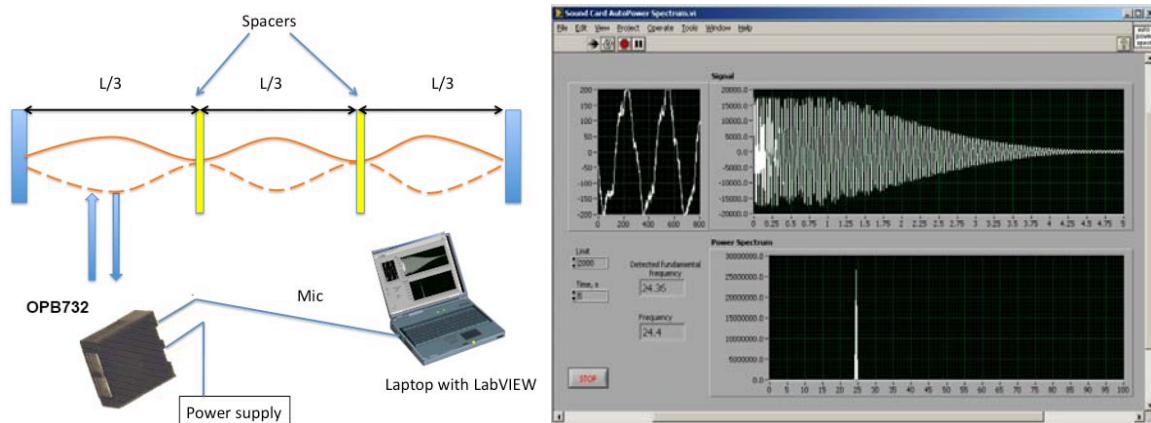


Figure 41. Set-up for straw tension measurement (left) and the LabVIEW control panel with the input signal from the OPB732 and the Fourier spectra (right).

#### 1.1.5.1.5 The Measurement of the Straw Straightness

Once the straws are fixed at both ends in the detector frame, the straightness is measured layer by layer with two light sources and a CCD camera/microscope. The two laser diodes illuminate the straw and the camera/microscope takes a photograph of the straw section. The system is calibrated using a wire stretched from top to bottom parallel to the straws. A stepper motor moves the camera and a picture is taken at 10 equidistant positions along the straw. A dedicated LabVIEW® program transforms the pictures into a black and white image and finds the two straw edges automatically. The program then calculates the positions of the straw centre (straightness) in the xy-plane and the diameter of the straw.

#### 1.1.5.1.6 Wiring

A gold-plated Tungsten wire from Toshiba with a diameter of 30  $\mu\text{m}$  is chosen (8). The limit of elastic deformation has been measured to 150 g and the rupture occurs around 220 g. The nominal wire tension is set to 90 g (see 1.1.5.1.7). The detector is placed in horizontal position and the straw resistivity is measured. All straw diameters are measured and recorded in the logbook. The webs are

then installed and the ground circuit is fixed to the inside of the straw with the help of the connection plug. A tight fit is necessary to ensure a good electrical contact. The ground petals are formed with a special tool to facilitate the insertion of the PEI plugs. A 0.1mm diameter wire ("needle" wire) is blown through the straw. The 30  $\mu\text{m}$  wire is fastened to the needle wire and kept under a small tension at all times during installation to avoid kinks. The wire is gently pulled through the straw. From both sides, the 30 $\mu\text{m}$  wire is inserted in the copper tubes and the copper tubes are then inserted through the electronic circuit into the contact plugs. Once the wire is fixed to the web side, a 90g weight is suspended to the wire on opposite side and fixed. The electrical continuity between the two pins is checked as well as insulation between wire and straw (broken wire). After wiring one layer the wire tension is measured and a HV test is performed to measure the leak current, which should not exceed 1 or 2nA per high voltage group at 1600V.

#### 1.1.5.1.7 Measurement of Wire Tension

The full Straw Tracker contains a total of 7168 anode wires and the wire tension need to be verified during and after installation. The wire resonance frequency is close to 50 Hz for a tension 80 g and a wire length of 2200 mm. 50 Hz is close to the 220 V voltage supply and in order to avoid this frequency, the nominal wire tension was set to 90 g. The acceptable values of wire tension during the module production are between 85 and 95 g. The upper limit of 95 g is considered to be comfortably below the elastic limit of 150 g, while the lower limit is high enough to allow good operation of the straw. Electrical instability of the wire was found for tensions below 35 g. However, to minimize electrostatic deflections on the wire the lower limit is set to 85 g. The wire tension measurement principle is shown in Figure 42: wire oscillations are stimulated in an external magnetic field with the help of a current generator; the resonant frequency of the wire is measured (9).

The current induced on the wires will be amplified with a high-input impedance amplifiers and an input signal threshold (typically of about 1.5mV). Signals will be digitized by a PC based A/D board and the measured frequency will be translated into applied wire tension  $T$  (in grams) following the formula:

$$T = \frac{4 \times \mu \times L^2 \times \nu^2}{a}$$

where  $L$  is the free wire length in cm,  $\nu$  is frequency in Hz,  $\mu$  is the mass per unit length in g/cm and  $a$  the gravitational acceleration. Uncertainties in the measured tension arise from variations in the wire diameter and the length of the vibrating wire. The minimum uncertainty can be estimated to  $\sim 1\%$ . The readout electronics is connected to a cell of 16 straws and measures the main resonance vibration frequency of each wire. The magnetic field near the tested wire must be at least 100 Gauss. The operator can modify the parameters of the pulse generator and Fourier analysis on the Labview based computer panel. The tension of the wires will be measured during the stringing process itself and a final global wire-tension measurement of all wires in the module will be carried out before the next assembly step. The results of the measurement will be written to the production database. Loss of wire tension between module assembly at JINR and arrival to CERN can happen and hence the wire tension will be measured again after delivery to CERN. Major attention will be paid to wires, which show a tension loss of more than 10 g. These wires will be investigated carefully and replaced if necessary .

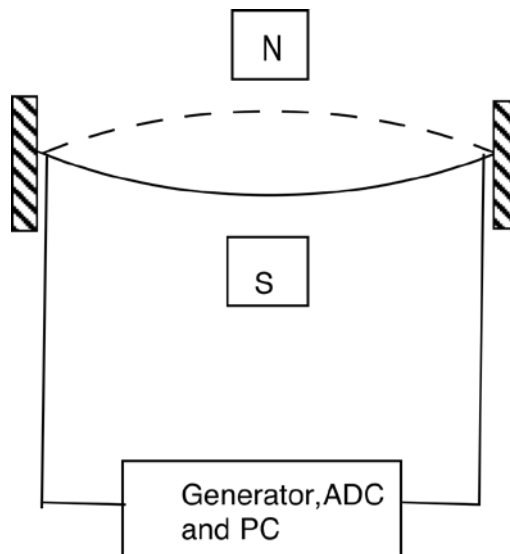


Figure 42. Schematic view of the wire tension measurement device.

#### 1.1.5.1.8 Gas Tightness Tests

The next stage will be to verify the glued joints between straws and the frame. It is important to perform this test at this stage because the straws and their glued joints to the straw support frame are still easily accessible and repairable in case of problem. A dedicated gas-tightness set-up is to be used to verify the quality of the about 2000 glue joints (per module) between the straws and their end plugs and between the end plugs and the straw support frame. The set-up used for the leak test consists of a flat steel table and a cover (see Figure 43). The system contains a temperature sensor, pressure gauges, vacuum stand and a system of valves and pipes. The inner module flange with a groove for the O-ring will be put on the flat table. The cover must be centred with respect to groove with the O-ring on the outer module flange. The module gas tightness will be achieved by the vacuum inside the module and with the help of 12 bolts that clamp the table and cover.

Straws and gas manifolds will be filled with Ar/CO<sub>2</sub> from a bottle with 20 mbar over atmosphere pressure. The vacuum volume of the module to be tested is about 1 m<sup>3</sup>. The leak rate (mbar•l/sec) will be evaluated by measuring the pressure increase of the vacuum around the straws as a function of time, once the pump has been stopped. A module will be approved for subsequent assembly whenever the measured leak rate does not exceed 10<sup>-2</sup> mbar•l/sec. Nevertheless, all effort will be made to get a value as low as possible (9).

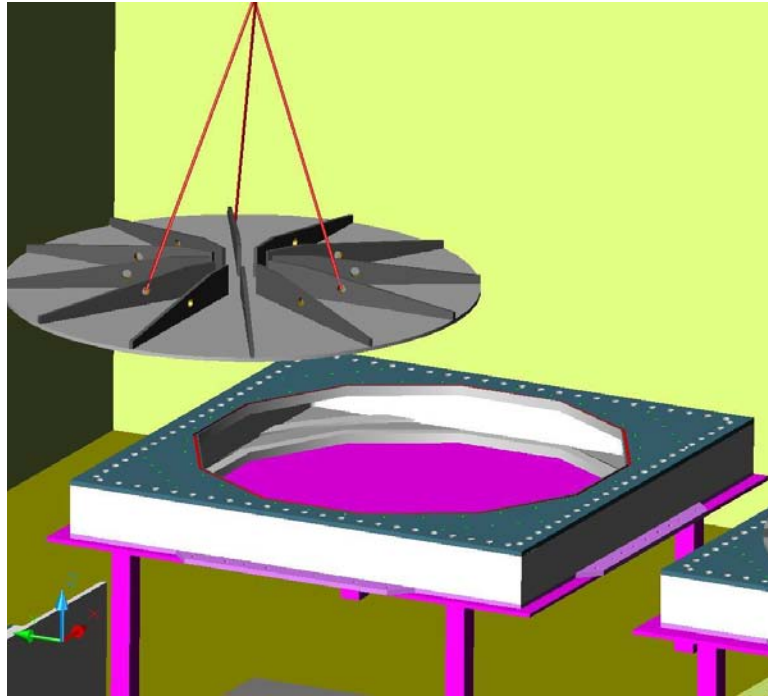


Figure 43. Flat steel table and a cover for module vacuum test.

#### 1.1.5.1.9 Gas tightness of the Module

The module includes about 500 straws and gas manifolds (see 1.1.5.1.1) with total gas volume about 110 l. The gas tightness test of assembled module will be carried out by measuring the pressure drop in the closed detector gas system filled with Ar/CO<sub>2</sub> at the over pressure about 1 bar. The minimum test duration will be not less than 20 hours. Internal pressure, atmospheric pressure and temperature will be recorded during this test. The recorded data (temperature and atmospheric pressure) will be used to correct the module gas system pressure drop. The leak rate (mbar/l/s) is calculated from the measured pressure drop over time. A module will be considered valid for installation whenever the measured leak rate of the module gas system does not exceed 100 mbar per 24 h at P=2 bar (about 4 cm<sup>3</sup>/min). The expected gas leak of 500 straws will be about 10 times lower.

#### 1.1.6 Frontend Electronics

The NA62 straw detector is a gaseous detector consisting of 7'168 drift tubes, 2.1 meter long, organized in 4 chambers, each station having 4 views. It aims at providing tracking information with a good resolution and a charged particle veto signal. The drift time measurement performed on the front-end electronics is indispensable for good tracking resolution. After analog processing of the straw signal, only timing information (start and end of the signal) is measured. From an electronics point of view, the following requirement can be defined:

- 130μm resolution for a single straw, 80μm for the detector
- Efficiency close to 100% (95% in high rate environment)
- Low noise
- Mean particle rate 40kHz, for straws close to beam up to 0.5MHz



### 1.1.6.1 Signal Parameters, Processing and Straw Properties

The basic detecting element is a straw drift tube of  $\sim 10$ mm diameter, 2.1 meter long. The cathode is formed by a very thin layer of copper and gold, few hundred atomic layers thick, so the electrical properties are determined by surface effects (one does not need to consider the skin effect). Indeed, the measured DC resistivity of the cathode is  $\sim 70$  Ohms (2.1 m) entirely determined by surface effects. The anode is  $30\mu\text{m}$  diameter gold plated tungsten wire. The straw can be considered as a very lossy transmission line and termination effects on both ends should be evaluated. With the gas mixture Ar/CO<sub>2</sub>(70/30), the electron total drift time is  $\sim 150$ ns.

As a response to each cluster of primary and secondary electrons created by the passage of particle, straw outputs a current signal with approximately hyperbolic shape and few microamperes amplitude. The shape differs from hyperbolic curve for the first few ns due to variable ion mobility. Also, when the selected gas would contain electronegative components, like CF<sub>4</sub><sup>3</sup>, the signal is distorted and of smaller amplitude due to electron attachment. The leading edge of the signal is very fast, of the order of 1ns, the trailing edge time depends on a number of factors like geometry, gas and voltage applied. The ion tail lasts up to few 100 $\mu\text{s}$  of microseconds. The electrical properties of the straws are the following:

- Characteristic impedance 350 Ohms (calculated) at 20MHz, 1000 Ohms at 1MHz
- Capacitance 23 pF
- Attenuation 2.3 at 20 MHz

The on-detector electronics consists of an 8-channel analogue front-end chip containing a fast preamplifier, semi-gaussian shaper, a tail cancellation circuitry, base line restorer and a discriminator. Input impedance of the preamplifier is a compromise between good straw impedance matching and a small crosstalk. The lower value is advantageous as it guarantees lower crosstalk and signal enhancement due to current increase during signal reflection on low termination impedance. The reflected signal, which returns after travelling to the far end of the straw and being reflected there, is already strongly attenuated and does not contribute significantly to the output. The shaping time should be short in order to get a response from the first primary cluster and thus better time resolution, but should be also sufficiently long to integrate further clusters so that there is only a single output pulse per particle crossing straw. Assuming 0.3mm average spacing between primary clusters, the shaping time should be much longer than 15ns for slow gas and 6ns for fast gas.

The ion tail cancellation is of utmost importance for straws with high rate of particles. Pile-up at high particle rate would cause loss of both efficiency and time resolution.

As baseline for the frontend analog electronics it is proposed to use the CARIOCA chip developed for the LHCb muon chambers. However, given the relatively small number of channels, electronics built from discrete components could be used if none of these chips could provide optimal performance. The CARIOCA chip has a shaping time constant of 15ns, so its operation with NA62 straw detector must be verified. This will be done in the 2010 test beam with the 64-straw prototype.

---

<sup>3</sup> CF<sub>4</sub> is considered in the back-up gas mixture, i.e. CO<sub>2</sub>/iC<sub>4</sub>H<sub>10</sub>/CF<sub>4</sub> (80%/10%/10%)

### 1.1.6.2 Modularity and Readout

The frontend modularity is following straw smallest unit. There are 16 straws in the basic unit of gas, high voltage and readout. The outputs from discriminators are either directly fed to the on-board TDC or transmitted to external module with TDC. Study and on-going design confirms the possibility to integrate 16 TDCs with 1ns RMS resolution inside Field Programmable Gate Array (FPGA) chip together with time-stamping, serialization and readout protocol using high speed serial links. Both starts and ends of signal must be recorded. The falling edge (end) of signal is the same for all straws seeing the same particle (Figure 44) and can be used for time measurement validation or even as a crude time measurement. It is also ideal for building fast hardware trigger or veto for multiple charged tracks. The rising edge (start) of the signal is used for precise drift time measurement and the track position is calculated through known r-t dependence.

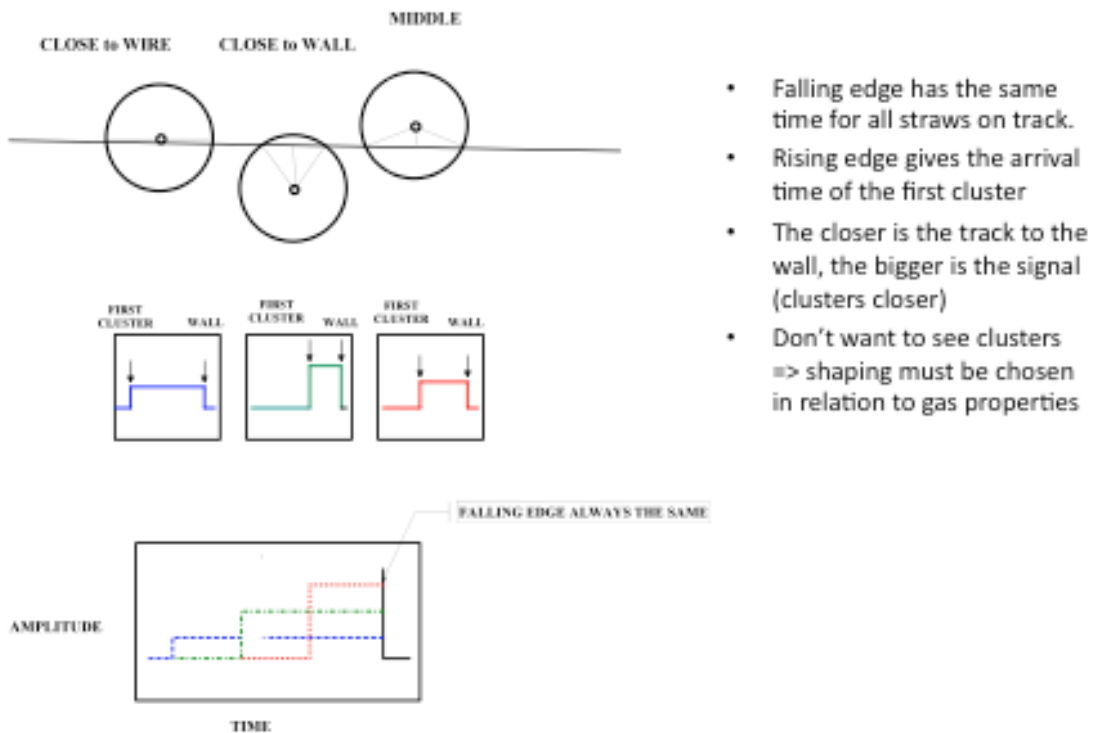


Figure 44: Timing of the straw detector.

### 1.1.6.3 Noise and Internal Crosstalk, Straw Termination

The threshold setting is a compromise between time resolution and the rate of noise hits. The lower the threshold, the better should be a time resolution and efficiency but the higher is the rate of noise hits. As the straw detector provides also multiple charged particles veto signal, the noise must be as small as possible. Crosstalk can also cause fake hits; multiple measures have been taken to reduce it as much as possible. For conductive crosstalk, the return paths of straw signals are separated already at the level of web connection and kept until frontend board input connector. Capacitive coupling effect can be mitigated by lowering input impedance of readout electronics and eventually by individual shielding of straw cathodes. Input impedance is the sum of preamplifier input impedance and input discharge protection resistor. The input impedance of the CARIOCA is about 50 Ohms at the working

frequency; the value of the protection resistor is of the order of 100 Ohms. The total load impedance for straw is thus  $\sim 150$  Ohms, to be compared with 350 Ohms straw characteristic impedance. The lower load impedance will cause signal reflections, but in a useful manner; it will increase the input current, thus enhancing input signal. As the straw is a transmission line with very high loss, the signal which returns after reflecting from the far end of straw, is already negligible. The other possibility considered for lowering capacitive crosstalk is covering straws from outside by very thin metallic layer connected separately to ground of the frontend board.

The straw far end is left open. This should enable for collecting as much charge as possible as the straw has a very high attenuation (2.3) at working frequency.

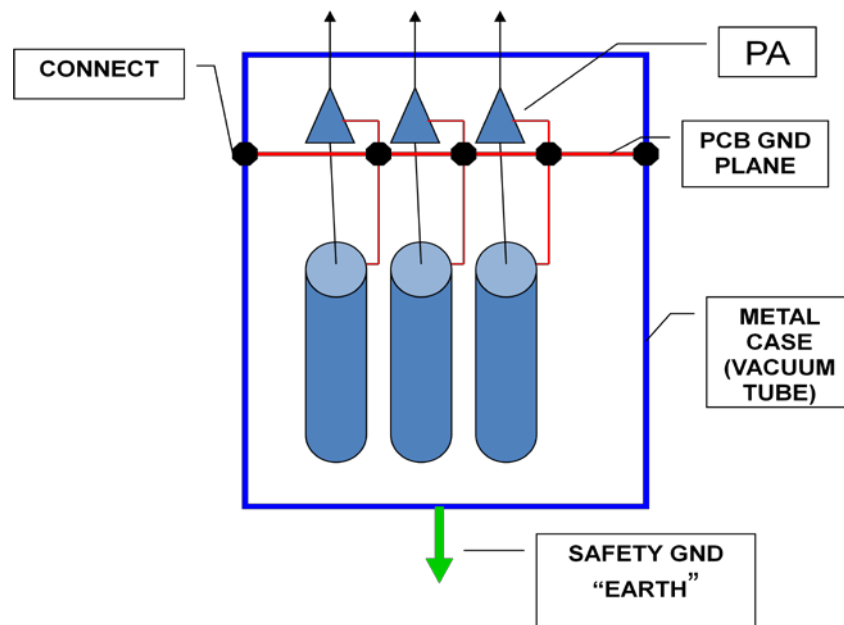


Figure 45: Grounding and shielding scheme

#### 1.1.6.4 External Crosstalk, Grounding and Shielding

External crosstalk is an interference with external objects surrounding the detector, like cranes, magnets, power supplies, wireless connections, etc. Another source can be caused by voltage potential difference between front and back end. One must also ensure connection of all conductive parts to safety ground. The proposed grounding and shielding scheme in Figure 45 ensures that the straw signal returns are separated and connected close to preamplifier inputs at frontend board level. This scheme was implemented in the 64-straw prototype.

The ground of the frontend board is connected around its perimeter to metal case, which is surrounding the whole detector, thus forming tight electromagnetic shield. Straws are connected to signal returns only on one end to prevent external currents flowing through the cathodes. All cable shields should be connected on both ends; one side directly to frontend board, backend side through damping impedance. If there are metallic pipes servicing gas or cooling, they should be electrically connected to metal frame as well.

The metal case of the station should be connected to safety earth at one point. The backend electronics (VME crates) must be connected to the same earth, thus providing both required safety connection and eliminates potential difference between frontend and backend electronics.

### 1.1.7 The Gas System

The gas system consists of two parts; first, the mixer system which delivers quantity, mixing ratio and pressure conditioning to downstream elements and secondly, the distribution system, which delivers the gas in well defined quantities to the individual detector components.

#### 1.1.7.1 Gas System Requirements

The total gas flow chosen correspond to a normal gas flow rate of  $\sim 2-4 \text{ cm}^3/\text{min}$  per straw. The gas modularity is optimised in order to minimise the number of lines between the detector and the distribution racks, and, on the other hand, to minimise the loss of performance in the case of an accidental leak in any module.

#### 1.1.7.2 The Mixer

The detector shall be supplied with a constant gas mixture of Ar/CO<sub>2</sub> (70%/30%) with a precision better than 1%. The total flow of the mixer will be 1500 l/h. Each primary gas line is equipped with a Digital Mass Flow controller to measure the component flow with appropriate accuracy. An output pressure regulator adjusts the downstream pressure from 0.2 to 2 bar. The control system provides a flow independent mixing ratio and adequate error handling. The mixer has to automatically follow the demand of the distribution system. The mixer system is in fact a standard mixing station of the LHC gas system project: a none-ATEX, two-gas mixer for a purged gas system with output pressure regulation (10).

#### 1.1.7.3 The Distribution

The gas from the mixer is distributed to four gas distribution racks, one for each chamber. The major design criteria of the distribution system is the uniform gas supply to each cell with adequate separation capabilities in case of pressure loss due to a leaking straw.

Figure 46 shows an overview of the entire gas system and Figure 47 the gas channel allocation of one chamber. Each chamber has four views, each containing 448 straws or 30 gas channels (Each view consists of 2x15 gas channels<sup>4</sup> and each channels supplies 16 straws). The gas distribution of one layer is split into 13 “normally flushed cells” and two “highly flushed cells” for the centre beam region. The 13 low flow cells per layer are grouped into one gas channel. The remaining two high-flow cells in the centre of the layer are grouped with similar cells of all layers to one gas channel (2 cells x 4 layers). In this way, one chamber has eight gas channels with low flow rate and two gas channels with high flow rate. The gas volume of one cell is about 3 litres, which results in about 20 l/h ( 1/2 Volume exchange per hour) and 24 l/h ( 1 volume exchange per hour) for low and high flow respectively. The following main elements in the gas system layout have been identified (see Figure 46):

---

<sup>4</sup> Each view consists of 2x15 gas compartments, however due to the beam window the number of straws near the beam can be smaller.

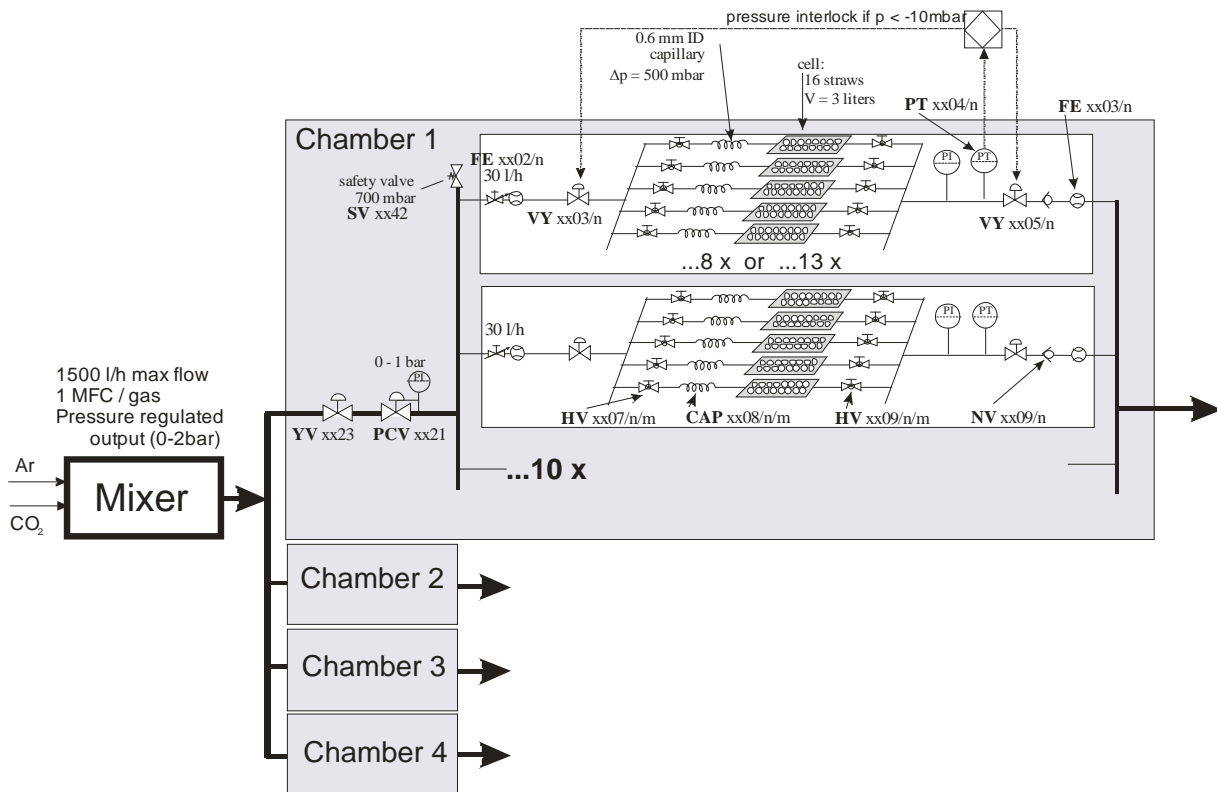


Figure 46. NA62 Straw Gas System overview.

The pressure regulator PCVxx21 (xx=61,62,63,64 for chamber 1,2,3,4) provides a constant relative pressure of 500 mbar to a gas manifold of 10 gas channels. The safety valve SVxx42 protects this manifold to about 700 mbar of over pressure. Each of the 10 gas channels is equipped with the following elements:

1. Input flow measurement FExx02/n (n=1,...,10)
2. Separation valves VYxx03/n and YVxx05/n
3. A gas distributor to 8 or 13 cells
4. Cell separation input valve HVxx07/n/m (m=1,...,8 or 13)
5. A capillary, CAPxx08/n/m, of 0.6mm inner diameter and a pressure drop of 500 mbar. The length of this capillary determines high or low flow rate for the cells.
6. Cell separation output valve HVxx09/n/m
7. Pressure transmitter PTxx04/n with interlock to VYxx03/n and VYxx05/n (fires in case less than 10 mbar under pressure is detected).
8. A non return valve, NVxx09/n, avoids backflow and therefore air contamination in case of pressure loss in a cell
9. Output flow measurement FExx03/n

The full functionality of the distribution system is covered by the standard LHC gas system control project.

As the straws will work in vacuum a protection system is required against a sudden leak in a straw. As shown above the modularity of the system (HV and gas) is 16 straws. PTxx04/n in combination with inlet and outlet shut-off valves VYxx03/n and YVxx05/n, assures a fast closure of the gas supply to one gas channel in case an under pressure is detected (e.g. broken straw). The contamination of the vacuum surrounding the straw tubes is therefore kept at a minimum. The non-return valve at the outlet of each gas channel will cause a slightly elevated straw pressure of 10 to 15 mbar above atmosphere.

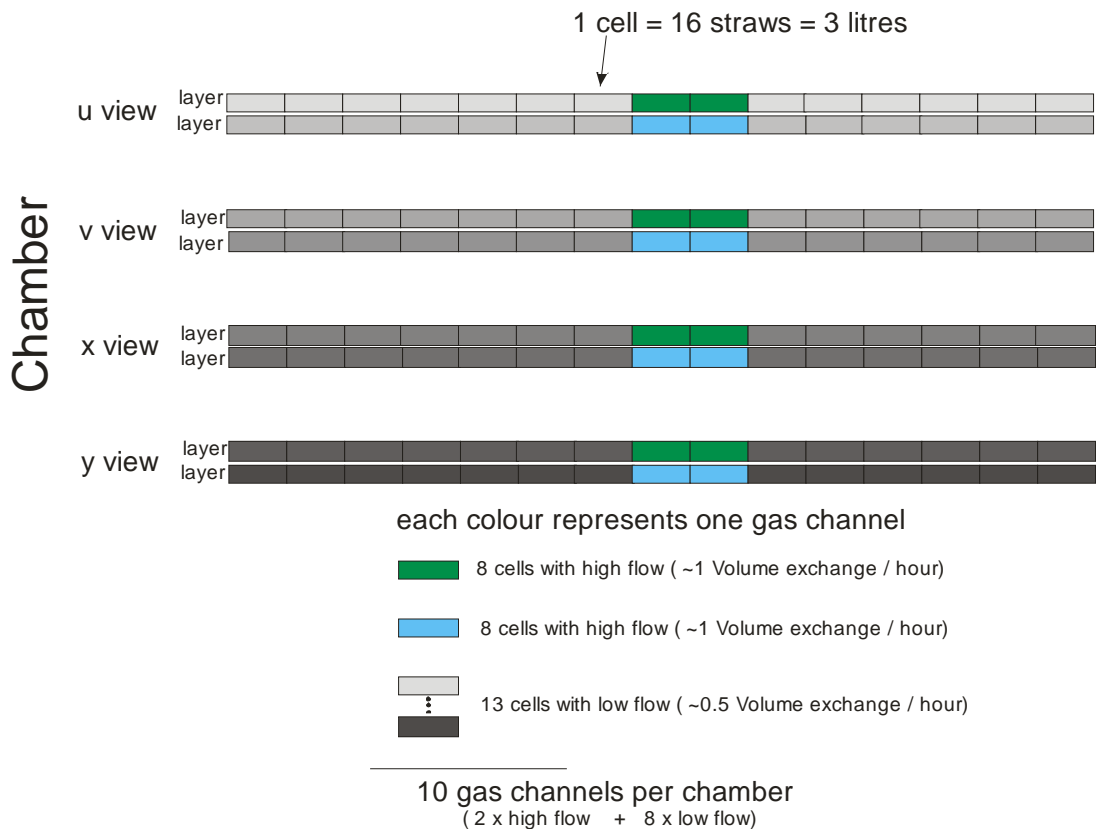


Figure 47. NA62 Straw Gas channel allocation.

### 1.1.8 Straw Tracker DCS

#### 1.1.8.1 DCS Architecture

The detector control system (DCS) should provide control and monitoring of the detector hardware. In addition, it should perform archiving of the hardware parameters to the database in order to provide access to this information during the off-line data analysis.

It has been decided to use the common DCS system, now under development at CERN, which is based on the PVSS II SCADA toolkit and the JCOP framework.

The Tracker controlled/monitored equipment includes the following items:

- Low voltage power supplies.

- High voltage power supplies.
- Gas mixing and distributing systems.
- Low voltage and temperature monitoring system.

#### 1.1.8.2 Low Voltage (LV) System

The LV system should provide power to the front-end (FE) boards placed on the four straw tracker chambers. Each chamber contains four views and each view contains 30 FE boards. In the present design, one FE board consumes  $\sim 1$  A at 5 volts and therefore one module requires the LV power supply to provide a current of about 30A at 5 V. These requirements could be fulfilled by eight Wiener power supplies MPV8008, which have eight channels of 10 A output current each. One view requires four channels and therefore, two power supplies will provide the required power for one chamber. The MPV8008 could be controlled in a similar way to the solution used in the LHC experiments. It includes a CAN-bus interface card and the OPC-server providing the interface to PVSS. A second possibility to control the MPV8008 is to use the TCP/IP protocol together with the corresponding TCP/IP PVSS driver which is part of the PVSS driver package. The final choice of the FE electronics and corresponding LV power supplies will be done once the results from the 2010 test beam with the 64-straw prototype is known.

#### 1.1.8.3 High Voltage System

The Straw tracker requires a high-voltage (HV) source with voltage below 2 kV and low current. The present design assumes two HV channels per view which gives 32 channels in total. The CAEN HV power supply board A1535, containing 24 channels with 3.5KV/3mA output, should be sufficient. To have 32 HV channels, two boards of this type housed in CAEN SY2527LC mainframe are needed. The mainframe should be controlled via Ethernet line with TCP/IP protocol and corresponding CAEN OPC server. The JCOP framework is suitable for the board A1535 and this component exists as it was developed for the CMS ME1/1 muon chambers.

#### 1.1.8.4 Gas System Controls

The gas system for the straw tracker should provide and distribute Ar/CO<sub>2</sub> gas mixture to individual straw cells (16 straws). The plan is to use the CERN standard gas mixing/distribution system based on PVSS with the possibility to control and monitor the gas mixing and gas flow values from the DCS PC. For this purpose PVSS distribution manager will be used. Both software and hardware interlock signals to prevent HV turning on in case of missing gas flow or incorrect gas mixture will be implemented.

Due to the fact that the straws are placed in vacuum, the gas system should rapidly close the gas line to a cell in case of a leak in a straw. Pressure sensors will detect a sudden drop in pressure on the supply lines. In this case, the gas system should also send a signal to the Straw Tracker DCS to switch off the corresponding HV channels or the whole HV system.

#### 1.1.8.5 Thermometry and FE monitoring

In order to get information about the cover (front-end) temperature at the straw group inlet, one thermo-sensor per FE cover will be mounted. Two voltages one the FE boards and the current consumed by a board will be measured using Embedded Local Monitoring Boards (ELMBs) (11).

A chamber view has 30 boards and four thermo-sensors will be mounted directly on the mechanics structure. In total, one view needs to measure 34 temperature values and 90 voltages. Therefore, to

read out all monitoring information from one chamber 10 ELMBs are needed. The readout should be performed via CAN-bus and OPC server, which is in a way similar to the monitoring of the LV power supply. It seems reasonable to have one CAN-bus branch per chamber, which gives in total four CAN-bus branches.

In case the LV power supplies control protocol is compatible with the ELMB control protocol, the LV power supplies will be connected to the chamber CAN-bus branches. The final decision depends on the final choice of the FE electronics.

#### 1.1.8.6 Logical Trees in DCS and FSM

To get a convenient way of navigation through the detector elements, the DCS logical tree should have a structure including both tracker nodes and gas system nodes. Due to the fact that the detector has only a few LV and HV channels, the bottom node of the tree should be linked to the corresponding channel of the LV or HV power supply in the hardware tree. The FSM tree should correspond to the Straw Tracker logical tree. The states of FSM should correspond to the states of the whole detector.

#### 1.1.8.7 DCS Development and Maintenance

The plan is to use our own DCS PC running tracker PVSS system and all detectors DCS OPC servers in one Windows-based computer. This PC should have CAN-bus adapter cards installed. After the development is finished and to simplify the maintenance of the detector DCS, the plan is to create a JCOP FW component containing all Tracker PVSS panels, scripts and port it to the NA62 Central DCS computer. A copy of this component should be stored in the NA62 DCS repository. The Tracker DCS PC should be used to run the DCS servers and to house the CAN-bus adapters. To simplify the control of the detector during further hardware development, debugging and maintenance, the PC to access PVSS panes located at the Central DCS PC, will be used. For this purpose the DCS PC should have a PVSS User Interface software installed.

### 1.1.9 Alignment and Installation

#### 1.1.9.1 Requirements

Alignment is the procedure in which the positions of the detector elements are determined. The residual uncertainties on these positions after the detector alignment has been performed are defined as the detector misalignments. Any misalignment of the elements of the detector will degrade the resolutions and the overall detector performance. The chambers will be equipped with eight reference points visible from the outside as shown in Figure 48. The reference points are positioned with respect to the straws with a precision of about 150  $\mu\text{m}$  and will be measured before the straws are inserted. The real position of the reference points will be measured after the assembly of the module structure, but before installation in the experiment. The main principles of the alignment strategy are:

- The holes for the straws are drilled with a precision of  $\sim 0.05$  mm
- The beams fixing the straws are positioned on the center plate (#1) of  $\sim 0.1$ mm
- The straws are assembled with a precision better than 0.1mm over their full length
- The positions of the straw holes are measured relative to the "targets" (red dots) with a precision better than 0.05 mm.



- Alignment with tracks: procedure to be defined
- Adjustable supports under each chamber for installation and alignment of the chambers.

### 1.1.10 Detector installation

In order to install the chambers, an interface part is connected on each side of the chamber. 16 bars interlink the two interface parts and will protect the chamber from axial forces as shown in Figure 48. Finite element calculations will determine the exact number and dimensions of these bars. Before the chambers are installed, the two modules are joined together. This operation is carried out after the two modules have passed the quality control at CERN.

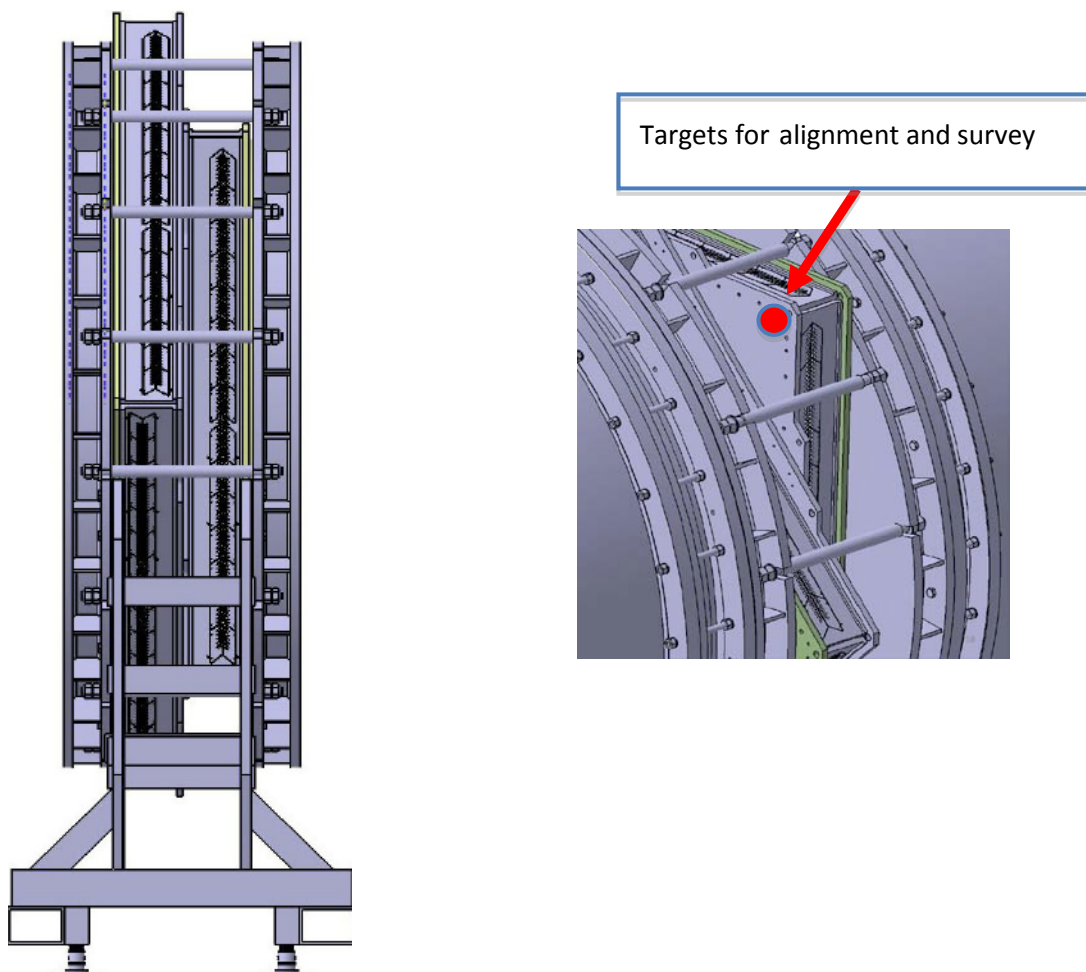


*Figure 48. 16 bars parallel to the beam connects the two interface parts and protect the chamber from axial forces (left) and detail of the connection to the blue tube. Eight reference points per chamber are for survey and alignment.*

### 1.1.11 The Assembly and Testing of a 64-straw Prototype

In order to validate the final design and assembly procedures, a full-length 64-straw prototype was built (12). The straw tracker prototype support was assembled and measured on a precise flat table using a height gauge with a precision of +/-10 microns. All reference holes were measured. A complete mapping of the prototype was recorded and used for the prototype realignment during all assembly steps (see Figure 49).



Figure 49. View of the prototype structure (left) and the measurement of the frame on the granite table.

#### 1.1.11.1 Installation and Alignment of the Straw Spacer

A full-scale low-density spacer for straws support was manufactured according to the principles explained in 1.1.5.1.3. Their position was adjusted on the prototype using the granite flat table taking into account their final position and including the deformation generated by gravity acting on the aluminium structure. The spacer in its final position with its dedicated adjustment tools is shown in Figure 50.

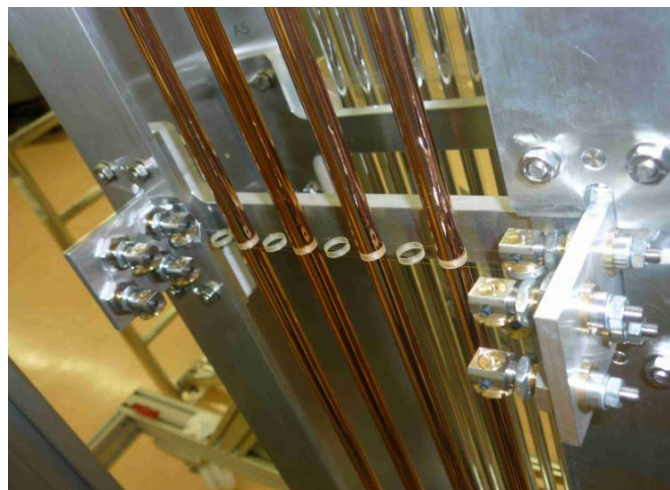


Figure 50. A view of four inserted straws supported by a spacer.

#### 1.1.11.2 Assembly Tooling

A dedicated tool was designed for the prototype assembly. This support allows to work in two different positions: horizontal for the straw insertion and straightness adjustment shown in Figure 51 and vertical for the final gluing under tension.

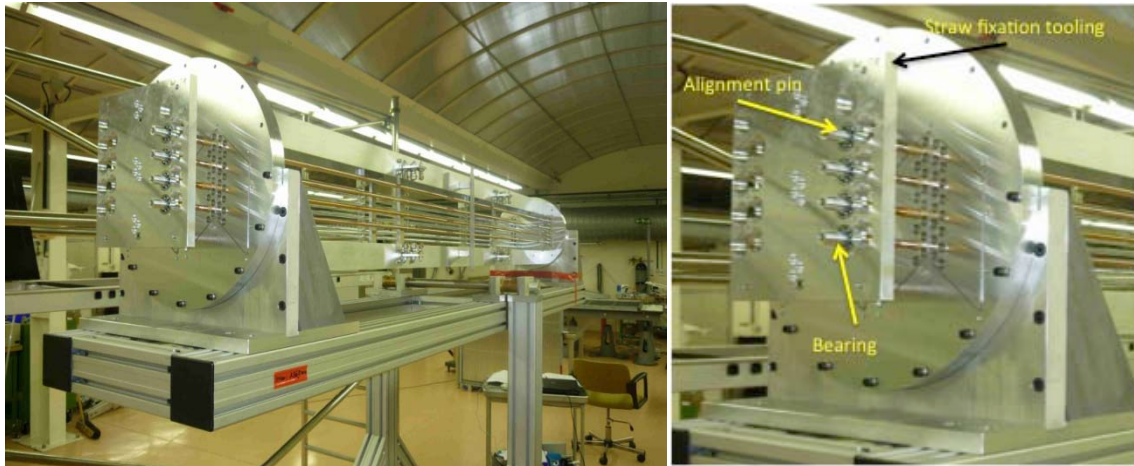


Figure 51. The prototype in the assembly tooling in horizontal position (left) and the straw fixation tooling (right).

### 1.1.11.3 Straw Insertion and Gluing

The PEI end plugs are then introduced and the alignment tooling support installed. Every straw is fixed with a dedicated pin inserted through a spherical bearing at both ends. The straw fixation tooling blocks the straw and guarantees the 1.5 kg pretension to the straws as shown in Figure 51 (right). The straw is free to move in the straw fixation plate, which guarantees the straightness of the straw after the curing of the glue. On the upper side, the linear translation is blocked, while, on the bottom side, the pin is allowed to slide through the bearing. A tension of 15N is put on the straws using a spring-loaded tool. On the bottom side, the end-plug groove is protected with an O-ring joint and a soft spring is inserted to maintain the end plug in the correct position during the gluing process as shown Figure 52 (left). Tra-bond 2115 epoxy resin is used to glue the straws and as its viscosity is very low the glue flows by capillarity. On the bottom side, the glue is applied to the outer diameter of the end plug before it is pushed gently vertically until it touches the aluminium plate. The soft spring maintain it in position. The glue is injected between the straw and the end-plug. On the top side, glue is applied to outer diameter of the end plug and it is gently slid vertically downwards till the aluminium end plate. The glue is then injected between the straw and the end plug as shown in see Figure 52 (right). After 24 hours of polymerisation, the alignment pins are removed and the alignment tool transferred to the next straw gluing position. The end plugs are then cut to a final length using a dedicated cutting device.



Figure 52. Bottom side gluing (left) and the gluing of the top side (right).

### 1.1.11.4 Straightness Measurement

After the assembly of the first layer, every straw tube position is measured with a CCD camera fixed to a height gauge. Seven positions are recorded for each tube, measured under a 2 bar absolute pressure. As final result, the straightness obtained on the fourth layer is shown in Figure 53. The precision in the spacer assembly is about  $\pm 35\mu\text{m}$  and the straightness is within  $\pm 100\mu\text{m}$  for each straw.

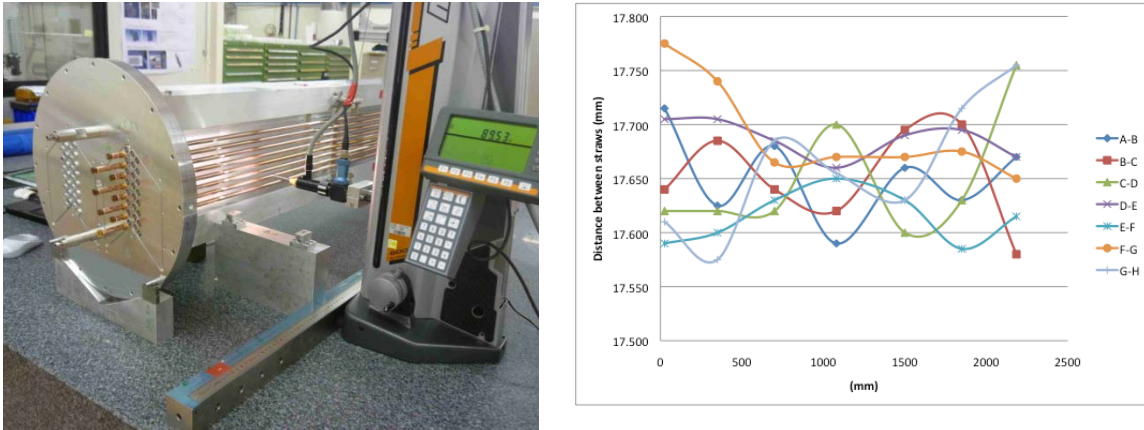


Figure 53. Measurement set up (left) and the distance between neighboring straws (right). The straws are kept at 2 bar absolute pressure <sup>5</sup>.

### 1.1.11.5 Straw Tension Measurement

As explained in 1.1.5.1.4, the straw tension is measured with a long distance reflective switch (OPB732). It measures the frequency once a smooth rod gently excites the straw. This method allows for a fast and accurate measurement of the resulting pretension in the straws after straw installation. The results for the first 32 straws are shown in Figure 54.

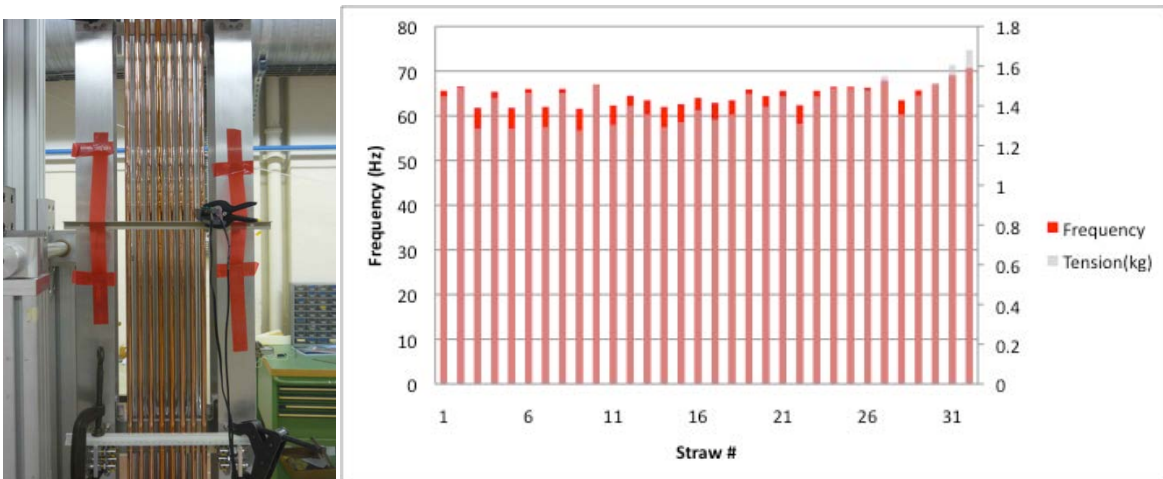


Figure 54. Set up in vertical position for straw tension measurements (left) and the measured tension (right).

<sup>5</sup> The distance between straws is 17.65 mm in the prototype. For the final chamber design it was changed to 17.6 mm.

### 1.1.11.6 Wiring Fixation option #1 (Crimping)

The detector is placed in horizontal position and the straw resistivity is measured. All straw diameters are measured and recorded in the logbook. The circuits (webs) are then installed and fixed. The ground petals (connects to the inside of the straw) are formed with a special tool to facilitate the insertion of PEI plugs. The wiring tool connected to a nitrogen bottle and a 0.1mm diameter needle wire is installed. The wire is blown through the straw as shown in Figure 55 (left). The 30 $\mu$ m anode wire is fixed to the needle wire. From this moment on, the 30 $\mu$ m wire must be kept under a small tension to avoid any kinks on the wire. The wire is gently pulled through the straw. From both sides, the anode wire is inserted in the copper crimp tubes. The crimp tubes are then inserted through the electronic circuit into the HV plugs. Once the wire is crimped on the web side with a special crimping tool, a 90g weight is attached to the wire on the opposite side before crimping the wire as shown in Figure 55 (right). The electrical continuity between the two pins is checked as well as the electrical insulation between wire and straw. Then, a complete high-voltage test is performed to measure the leak current, which should not exceed 1 or 2nA per high voltage group at 1600 V.

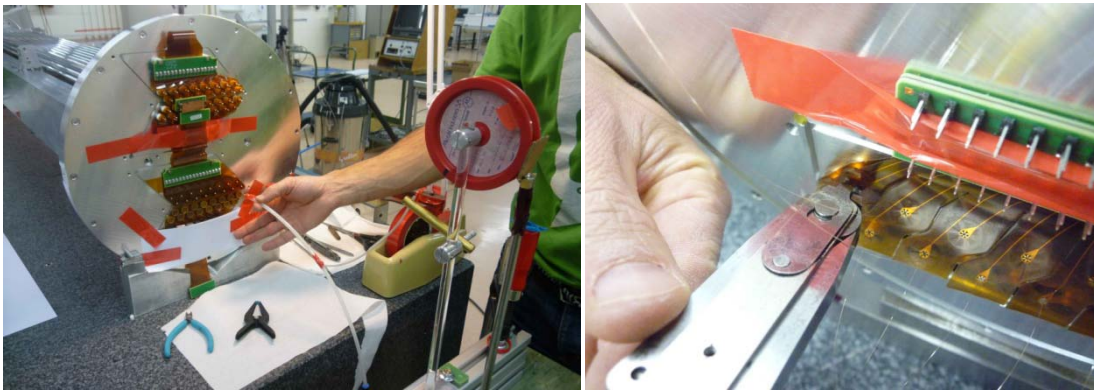


Figure 55. Blowing the wires (left) and crimping of the wire (right)

### 1.1.11.7 Wire Fixation option #2 (soldering).

A second method of positioning the wires was tested in the prototype. The principle of wire position is shown in Figure 56. An external tools was fixed on the flange reference holes by dowel pins. The accuracy of wire spacing with this method is  $\pm 5 \mu\text{m}$  and given by the precision in tooling. Each wire is blocked between 3 pins.

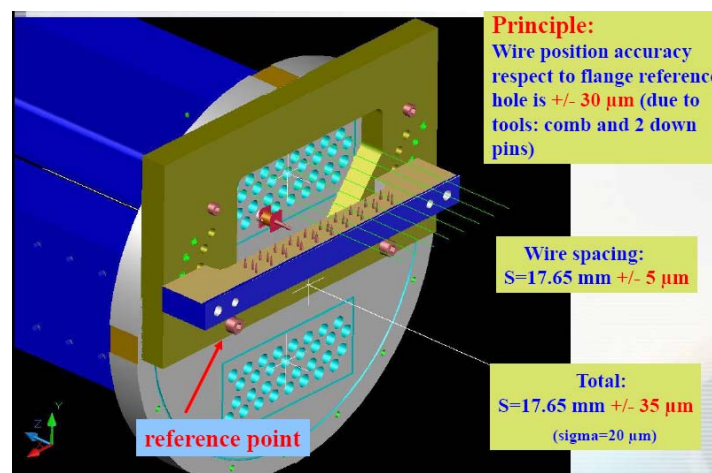


Figure 56. Wire positioning method

The method to verify the wire position at the straw ends during the assembly of the wires is shown in Figure 57.

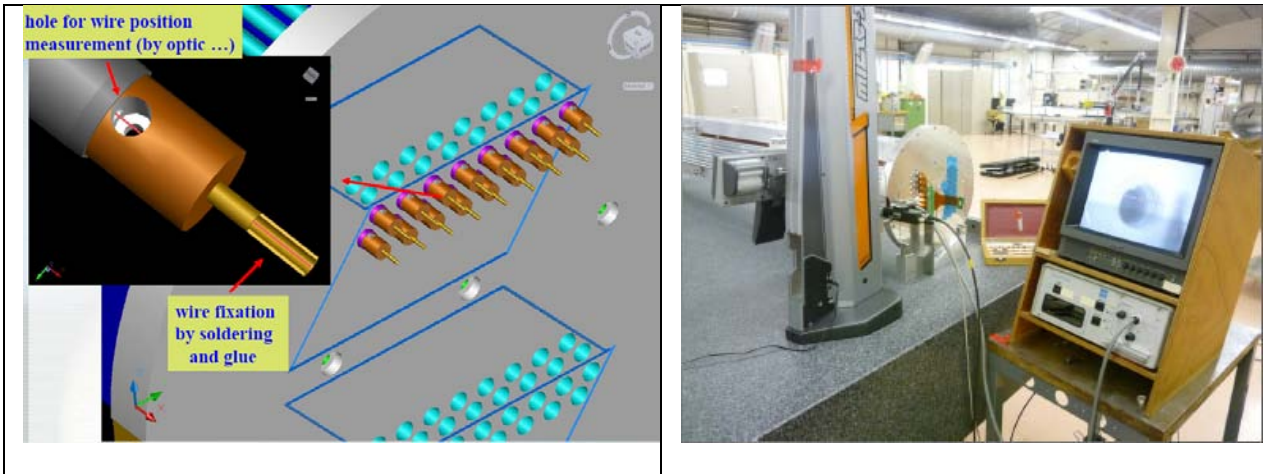


Figure 57. Verification scheme and measurement procedure

The measurements of the relative wire positions are presented in Figure 58. The values (distance between two neighbouring wires) showed that at least one of the two wires was badly positioned and it was replaced. The nominal value of the wire spacing is 17.65 mm. The wire positioning precision is +/- 35 μm, which includes a measurement accuracy of +/- 10 μm. σ of this distribution is about 10 μm and is negligible compared to the requirements (the straw spatial resolution should be better than σ=130 μm).

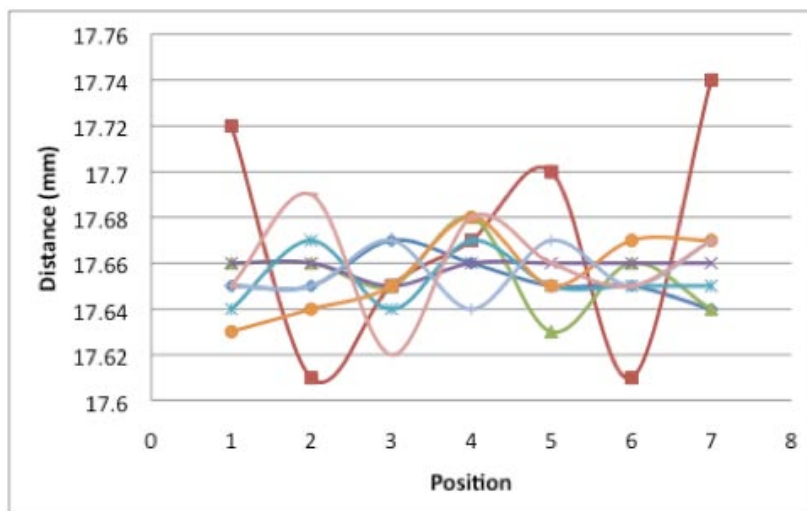


Figure 58. Measured wire positions for the soldered wires.

### 1.1.11.8 The Partitions

The dismantlable partitions are mounted after the wiring and HV check. Thanks to the dry mounting, they can be removed if necessary, e.g. to replace a wire or access a straw (see Figure 59). After the assembly of the partitions, the first leak tightness test takes place.

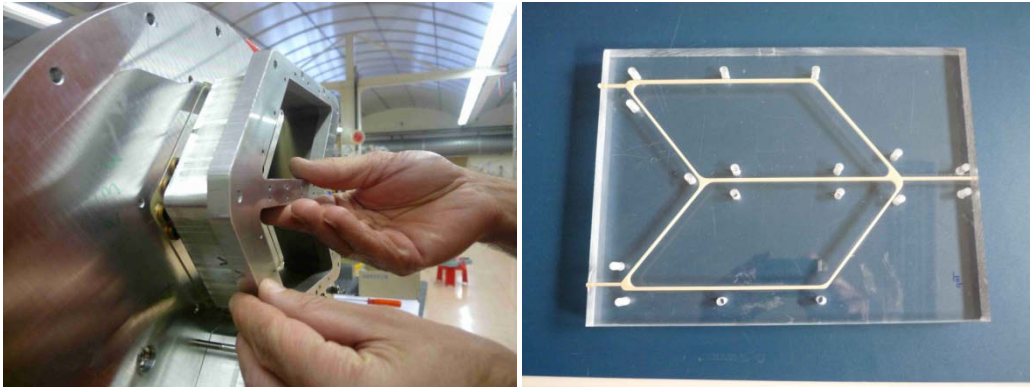


Figure 59. View of the cells partition during assembly (left) and polyurethane joint in the mould (right).

#### 1.1.11.9 Measurement of the Leak Rate

In order to test the straws in real working conditions a dedicated vacuum vessel was built. The prototype is directly fixed on the first edge, and fastened through a metallic bellows to the second end (see Figure 60). With a turbo pump we obtained a vacuum of  $2.5 \times 10^{-4}$  mbar. Through a window on the side of the tube, the centre of the first layer could be observed. No deflection or movement of the straws was noticed during this operation. The permeation tests, using Argon (70%) and CO<sub>2</sub> (30%), showed a total leak rate of  $9.3 \times 10^{-2}$  mbar l/s while the specification is  $10 \times 10^{-2}$  mbar l/s. The requirements and measurements are summarized in Table 3.



Figure 60. View of the far end with the metallic bellows for the vacuum and leak test. The two gas cells (without electronics) are visible in the center.

Table 3. NA62 gas load

Straw detector at NPT (measurement)		LAV (estimate)	Blue tube (estimate)
Single straw	Full detector (7168 straws)		
0.82 mbar cm <sup>3</sup> /min	$9.8 \times 10^{-2}$ mbar l/s	$3 \times 10^{-2}$ mbar l/s	$2 \times 10^{-2}$ mbar l/s

### 1.1.11.10 Aging studies

In order to validate the different components and material in the detector, a dedicated prototype was built. The prototype contains two straws; one with Aluminium coating and with Copper/Gold (see 1.1.3.1). The straw end-pieces were made from ULTEM and the connection to the straws was made with a section of the web (see 1.1.5.1.1). The wire is the 30  $\mu\text{m}$  gold plated Tungsten from Toshiba foreseen for the chamber production. Final crimp tubes were used for electrical and mechanical connections of the wire to the web. The prototype was mounted in the CERN aging test facility. A gas mixture of 70% Argon and 30% was used. The parameters during the aging test are summarized in Table 4.

Table 4: Parameters for the aging test-up

Gas mixture	Gas flow	Current	Total charge	Irradiation area	High voltage	Fe <sup>55</sup> -scan slit size
Ar(70%) CO <sub>2</sub> (30%)	0.5 cm <sup>3</sup> /min	280 nA	0.27 C/cm (500h)	10 mm	1700 V	1 mm

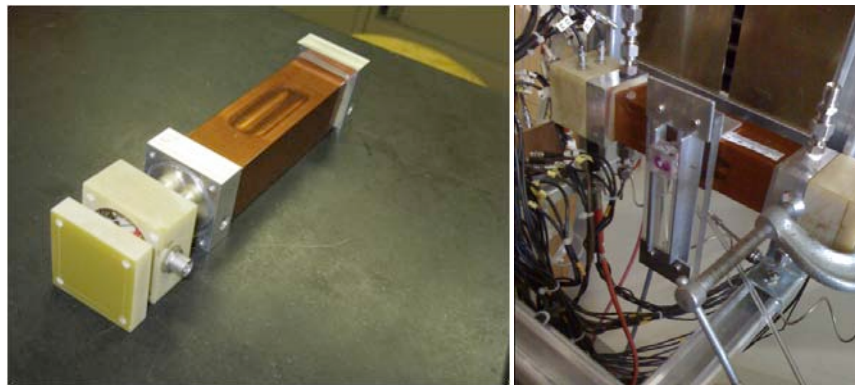
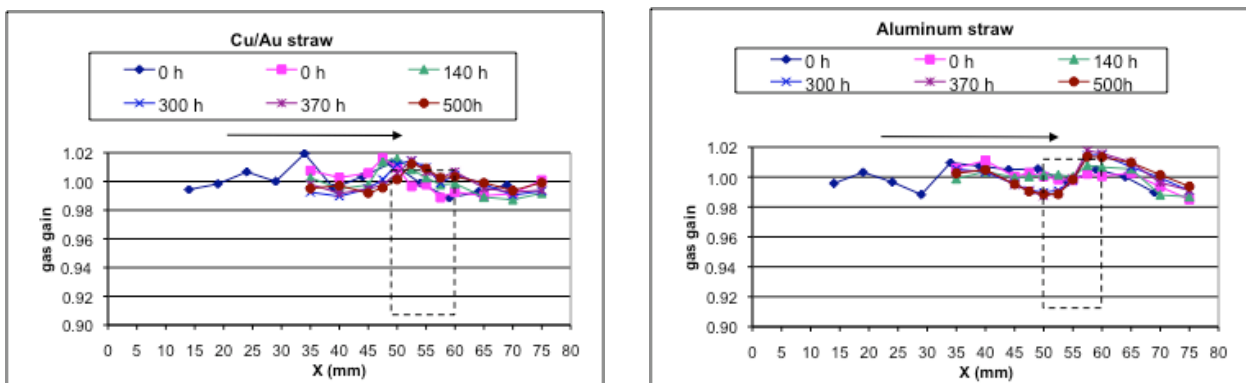


Figure 61. Straw prototype for material validation (left) and mounted in the set-up (right)

A scan with a Fe<sup>55</sup> source is made at intermediate irradiation levels over the window from 10 to 75 mm (13). The results are shown in Figure 62 and no change in amplitude can be seen up to a total charge of 0.27 C/cm. The estimated accumulated charge for the hottest straws in the experiment is 0.04 C/cm. After the initial run with Ar/CO<sub>2</sub> it was decided to dismount the prototype and investigate the wire and the inside of straw surface around the irradiated region.

Figure 62. Amplitude scan. for the Cu/Au straw and Aluminium straw respectively.





## Bibliography

1. **NA62 Collaboration Ambrosino F. et al.** NA62 Status Report. *CERN-SPSC-2007-035*.
2. **B. Hallgren et al.** For the CPD (Calorimeter Pipeline Digitizer module) see: The NA48 LKr calorimeter digitizer electronics chain - Wire Chamber Conference 1998, Vienna. *CERN preprint EP/98-48*. 1998.
3. *Straw Tracker Prototype for the precise measurement of very rare decay  $K \rightarrow \pi + nn$* . **Movchan, Sergei**. Glasgow : PSD8, 2008. 8th. International Conference on POsition Sensitive Detectors. Vol. 604, pp. 307-309.
4. **Blum, W., Riegler, W. and Rolandi, L.** *Particle Detection with Drift Chambers*. 2nd. Berlin : Springer, 2008.
5. **Catianccio, Andrea**. PIPES UNDER INTERNAL PRESSURE AND BENDING. *CERN PH-EP-Tech-Note-2009-004*.
6. *Development of the CARIOCA front-end chip for the LHCb muon detector*. **Bonivento, W., et al.** 1-2, P233, s.l. : NIM A, 2002, Vol. 491.
7. **Moraes, D. et al.** The CARIOCA Front End Chip for the LHCb muon chambers. *Internal Note LHCb-MUON 2003-009*.
8. **Romaniouk, Anatoli**. *Toshiba wire validation*. s.l. : <https://edms.cern.ch/document/113748/1>.
9. **Dorovich D. et al.** Device for measuring of wire tension in drift tubes. *JINR, 2001, P13- 2001-201, 11 p.*
10. **WASEM, Albin**. *Two Gas Single Pass Mixer*. CERN. Geneva : <https://edms.cern.ch/document/459759/1>.
11. **Burckhart, Helfried**. ELMB. *CERN*. [Online] <http://elmb.web.cern.ch/ELMB/ELMBhome.html>.
12. **Danielsson, Hans**. Procedures and test results from the assembly of the 64-straw prototype. *CERN*. [Online] <https://edms.cern.ch/document/1085111/1>.
13. *Aging studies for the ATLAS Transition Radiation Tracker (TRT)*. **T. Akesson et al.** 1-2, December 2003, Nuclear Instruments and Methods in Physics Research Section A: Accelerators, Spectrometers, Detectors and Associated Equipment, Vol. 515, pp. 166-179.